

5 Low-energy constants

In the study of the quark-mass dependence of QCD observables calculated on the lattice, it is common practice to invoke chiral perturbation theory (χ PT). For a given quantity this framework predicts the nonanalytic quark-mass dependence and it provides symmetry relations among different observables. These relations are best expressed with the help of a set of linearly independent and universal (i.e. process-independent) low-energy constants (LECs), which appear as coefficients of the polynomial terms (in m_q or M_π^2) in different observables. When numerical simulations are done at heavier than physical (light) quark masses, χ PT is usually invoked in the extrapolation to physical quark masses.

5.1 Chiral perturbation theory

χ PT is an effective field theory approach to the low-energy properties of QCD based on the spontaneous breaking of chiral symmetry, $SU(N_f)_L \times SU(N_f)_R \rightarrow SU(N_f)_{L+R}$, and its soft explicit breaking by quark-mass terms. In its original implementation, in infinite volume, it is an expansion in m_q and p^2 with power counting $M_\pi^2 \sim m_q \sim p^2$.

If one expands around the $SU(2)$ chiral limit, there appear two LECs at order p^2 in the chiral effective Lagrangian,

$$F \equiv F_\pi \Big|_{m_u, m_d \rightarrow 0} \quad \text{and} \quad B \equiv \frac{\Sigma}{F^2}, \quad \text{where} \quad \Sigma \equiv -\langle \bar{u}u \rangle \Big|_{m_u, m_d \rightarrow 0}, \quad (71)$$

and seven at order p^4 , indicated by $\bar{\ell}_i$ with $i = 1, \dots, 7$. In the analysis of the $SU(3)$ chiral limit there are also just two LECs at order p^2 ,

$$F_0 \equiv F_\pi \Big|_{m_u, m_d, m_s \rightarrow 0} \quad \text{and} \quad B_0 \equiv \frac{\Sigma_0}{F_0^2}, \quad \text{where} \quad \Sigma_0 \equiv -\langle \bar{u}u \rangle \Big|_{m_u, m_d, m_s \rightarrow 0}, \quad (72)$$

but ten at order p^4 , indicated by the capital letter $L_i(\mu)$ with $i = 1, \dots, 10$. These constants are independent of the quark masses,¹ but they become scale dependent after renormalization (sometimes a superscript r is added). The $SU(2)$ constants $\bar{\ell}_i$ are scale independent, since they are defined at scale $\mu = M_\pi$ (as indicated by the bar). For the precise definition of these constants and their scale dependence we refer the reader to Refs. [1, 2].

If the box volume is finite but large compared to the Compton wavelength of the pion, $L \gg 1/M_\pi$, the power counting generalizes to $m_q \sim p^2 \sim 1/L^2$, as one would assume based on the fact that $p_{\min} = 2\pi/L$ is the minimum momentum in a finite box. This is the so-called p -regime of χ PT. It coincides with the setting that is used for standard phenomenologically oriented lattice-QCD computations, and we shall consider the p -regime the default in the following. However, if the pion mass is so small that the box-length L is no longer large compared to the Compton wavelength that the pion would have, at the given m_q , in infinite volume, then the chiral series must be reordered. Such finite-volume versions of χ PT with correspondingly adjusted power counting schemes, referred to as ϵ - and δ -regime, are described in Secs. 5.1.4 and 5.1.5, respectively.

¹More precisely, they are independent of the 2 or 3 light quark masses which are explicitly considered in the respective framework. However, all low-energy constants depend on the masses of the remaining quarks s, c, b, t or c, b, t in the $SU(2)$ and $SU(3)$ framework, respectively, although the dependence on the masses of the c, b, t quarks is expected to be small.

Lattice calculations can be used to test if chiral symmetry is indeed spontaneously broken along the path $SU(N_f)_L \times SU(N_f)_R \rightarrow SU(N_f)_{L+R}$ by measuring nonzero chiral condensates and by verifying the validity of the GMOR relation $M_\pi^2 \propto m_q$ close to the chiral limit. If the chiral extrapolation of quantities calculated on the lattice is made with the help of fits to their χ PT forms, apart from determining the observable at the physical value of the quark masses, one also obtains the relevant LECs. This is a very important by-product for two reasons:

1. All LECs up to order p^4 (with the exception of B and B_0 , since only the product of these times the quark masses can be estimated from phenomenology) have either been determined by comparison to experiment or estimated theoretically, e.g. in large- N_c QCD. A lattice determination of the better known LECs thus provides a test of the χ PT approach.
2. The less well-known LECs are those which describe the quark-mass dependence of observables – these cannot be determined from experiment, and therefore the lattice, where quark masses can be varied, provides unique quantitative information. This information is essential for improving phenomenological χ PT predictions in which these LECs play a role.

We stress that this program is based on the nonobvious assumption that χ PT is valid in the region of masses and momenta used in the lattice simulations under consideration, something that can and should be checked. In the end one wants to compare lattice and phenomenological determinations of LECs, much in the spirit of Ref. [3]. An overview of many of the conceptual issues involved in matching lattice data to an effective field theory framework like χ PT is given in Refs. [4–6].

The fact that, at large volume, the finite-size effects, which occur if a system undergoes spontaneous symmetry breakdown, are controlled by the Nambu-Goldstone modes, was first noted in solid state physics, in connection with magnetic systems [7, 8]. As pointed out in Ref. [9] in the context of QCD, the thermal properties of such systems can be studied in a systematic and model-independent manner by means of the corresponding effective field theory, provided the temperature is low enough. While finite volumes are not of physical interest in particle physics, lattice simulations are necessarily carried out in a finite box. As shown in Refs. [10–12], the ensuing finite-size effects can be studied on the basis of the effective theory – χ PT in the case of QCD – provided the simulation is close enough to the continuum limit, the volume is sufficiently large and the explicit breaking of chiral symmetry generated by the quark masses is sufficiently small. Indeed, χ PT represents a useful tool for the analysis of the finite-size effects in lattice simulations.

In the remainder of this subsection we collect the relevant χ PT formulae that will be used in the two following subsections to extract $SU(2)$ and $SU(3)$ LECs from lattice data.

5.1.1 Quark-mass dependence of pseudoscalar masses and decay constants

A. $SU(2)$ formulae

The expansions² of M_π^2 and F_π in powers of the quark mass are known to next-to-next-to-leading order (NNLO) in the $SU(2)$ chiral effective theory. In the isospin limit, $m_u = m_d = m$,

²Here and in the following, we stick to the notation used in the papers where the χ PT formulae were established, i.e. we work with $F_\pi \equiv f_\pi/\sqrt{2} = 92.2(1)$ MeV and $F_K \equiv f_K/\sqrt{2}$. The occurrence of different normalization conventions is not convenient, but avoiding it by reformulating the formulae in terms of f_π , f_K is not a good way out. Since we are using different symbols, confusion cannot arise.

the explicit expressions may be written in the form [13]

$$\begin{aligned} M_\pi^2 &= M^2 \left\{ 1 - \frac{1}{2} x \ln \frac{\Lambda_3^2}{M^2} + \frac{17}{8} x^2 \left(\ln \frac{\Lambda_M^2}{M^2} \right)^2 + x^2 k_M + \mathcal{O}(x^3) \right\}, \\ F_\pi &= F \left\{ 1 + x \ln \frac{\Lambda_4^2}{M^2} - \frac{5}{4} x^2 \left(\ln \frac{\Lambda_F^2}{M^2} \right)^2 + x^2 k_F + \mathcal{O}(x^3) \right\}. \end{aligned} \quad (73)$$

Here the expansion parameter is given by

$$x = \frac{M^2}{(4\pi F)^2}, \quad M^2 = 2Bm = \frac{2\Sigma m}{F^2}, \quad (74)$$

but there is another option as discussed below. The scales Λ_3, Λ_4 are related to the effective coupling constants $\bar{\ell}_3, \bar{\ell}_4$ of the chiral Lagrangian at scale $M_\pi \equiv M_\pi^{\text{phys}}$ by

$$\bar{\ell}_n = \ln \frac{\Lambda_n^2}{M_\pi^2}, \quad n = 1, \dots, 7. \quad (75)$$

Note that in Eq. (73) the logarithms are evaluated at M^2 , not at M_π^2 . The coupling constants k_M, k_F in Eq. (73) are mass-independent. The scales of the squared logarithms can be expressed in terms of the $\mathcal{O}(p^4)$ coupling constants as

$$\begin{aligned} \ln \frac{\Lambda_M^2}{M^2} &= \frac{1}{51} \left(28 \ln \frac{\Lambda_1^2}{M^2} + 32 \ln \frac{\Lambda_2^2}{M^2} - 9 \ln \frac{\Lambda_3^2}{M^2} + 49 \right), \\ \ln \frac{\Lambda_F^2}{M^2} &= \frac{1}{30} \left(14 \ln \frac{\Lambda_1^2}{M^2} + 16 \ln \frac{\Lambda_2^2}{M^2} + 6 \ln \frac{\Lambda_3^2}{M^2} - 6 \ln \frac{\Lambda_4^2}{M^2} + 23 \right). \end{aligned} \quad (76)$$

Hence by analysing the quark-mass dependence of M_π^2 and F_π with Eq. (73), possibly truncated at NLO, one can determine³ the $\mathcal{O}(p^2)$ LECs B and F , as well as the $\mathcal{O}(p^4)$ LECs $\bar{\ell}_3$ and $\bar{\ell}_4$. The quark condensate in the chiral limit is given by $\Sigma = F^2 B$. With precise enough data at several small enough pion masses, one could in principle also determine Λ_M, Λ_F and k_M, k_F . To date this is not yet possible. The results for the LO and NLO constants will be presented in Sec. 5.2.

Alternatively, one can invert Eq. (73) and express M^2 and F as an expansion in

$$\xi \equiv \frac{M_\pi^2}{16\pi^2 F_\pi^2}, \quad (77)$$

and the corresponding expressions then take the form

$$\begin{aligned} M^2 &= M_\pi^2 \left\{ 1 + \frac{1}{2} \xi \ln \frac{\Lambda_3^2}{M_\pi^2} - \frac{5}{8} \xi^2 \left(\ln \frac{\Omega_M^2}{M_\pi^2} \right)^2 + \xi^2 c_M + \mathcal{O}(\xi^3) \right\}, \\ F &= F_\pi \left\{ 1 - \xi \ln \frac{\Lambda_4^2}{M_\pi^2} - \frac{1}{4} \xi^2 \left(\ln \frac{\Omega_F^2}{M_\pi^2} \right)^2 + \xi^2 c_F + \mathcal{O}(\xi^3) \right\}. \end{aligned} \quad (78)$$

³Notice that one could analyse the quark-mass dependence entirely in terms of the parameter M^2 defined in Eq. (74) and determine equally well all other LECs. Using the determination of the quark masses described in Sec. 3 one can then extract B or Σ . No matter the strategy of extraction, determination of B or Σ requires knowledge of the scale and scheme dependent quark mass renormalization factor $Z_m(\mu)$.

The scales of the quadratic logarithms are determined by $\Lambda_1, \dots, \Lambda_4$ through

$$\begin{aligned} \ln \frac{\Omega_M^2}{M_\pi^2} &= \frac{1}{15} \left(28 \ln \frac{\Lambda_1^2}{M_\pi^2} + 32 \ln \frac{\Lambda_2^2}{M_\pi^2} - 33 \ln \frac{\Lambda_3^2}{M_\pi^2} - 12 \ln \frac{\Lambda_4^2}{M_\pi^2} + 52 \right), \\ \ln \frac{\Omega_F^2}{M_\pi^2} &= \frac{1}{3} \left(-7 \ln \frac{\Lambda_1^2}{M_\pi^2} - 8 \ln \frac{\Lambda_2^2}{M_\pi^2} + 18 \ln \frac{\Lambda_4^2}{M_\pi^2} - \frac{29}{2} \right). \end{aligned} \quad (79)$$

B. $SU(3)$ formulae

While the formulae for the pseudoscalar masses and decay constants are known to NNLO for $SU(3)$ as well [14], they are rather complicated and we restrict ourselves here to next-to-leading order (NLO). In the isospin limit, the relevant $SU(3)$ formulae take the form [2]

$$\begin{aligned} M_\pi^2 &\stackrel{\text{NLO}}{=} 2B_0 m_{ud} \left\{ 1 + \mu_\pi - \frac{1}{3} \mu_\eta + \frac{B_0}{F_0^2} \left[16m_{ud}(2L_8 - L_5) + 16(m_s + 2m_{ud})(2L_6 - L_4) \right] \right\}, \\ M_K^2 &\stackrel{\text{NLO}}{=} B_0(m_s + m_{ud}) \left\{ 1 + \frac{2}{3} \mu_\eta + \frac{B_0}{F_0^2} \left[8(m_s + m_{ud})(2L_8 - L_5) + 16(m_s + 2m_{ud})(2L_6 - L_4) \right] \right\}, \\ F_\pi &\stackrel{\text{NLO}}{=} F_0 \left\{ 1 - 2\mu_\pi - \mu_K + \frac{B_0}{F_0^2} \left[8m_{ud}L_5 + 8(m_s + 2m_{ud})L_4 \right] \right\}, \\ F_K &\stackrel{\text{NLO}}{=} F_0 \left\{ 1 - \frac{3}{4} \mu_\pi - \frac{3}{2} \mu_K - \frac{3}{4} \mu_\eta + \frac{B_0}{F_0^2} \left[4(m_s + m_{ud})L_5 + 8(m_s + 2m_{ud})L_4 \right] \right\}, \end{aligned} \quad (80)$$

where m_{ud} is the common up and down quark mass (which may be different from the one in the real world), and $B_0 = \Sigma_0/F_0^2$, F_0 denote the condensate parameter and the pseudoscalar decay constant in the $SU(3)$ chiral limit, respectively. In addition, we use the notation

$$\mu_P = \frac{M_P^2}{32\pi^2 F_0^2} \ln \left(\frac{M_P^2}{\mu^2} \right). \quad (81)$$

At the order of the chiral expansion used in these formulae, the quantities μ_π , μ_K , μ_η can equally well be evaluated with the leading-order expressions for the masses,

$$M_\pi^2 \stackrel{\text{LO}}{=} 2B_0 m_{ud}, \quad M_K^2 \stackrel{\text{LO}}{=} B_0(m_s + m_{ud}), \quad M_\eta^2 \stackrel{\text{LO}}{=} \frac{2}{3} B_0(2m_s + m_{ud}). \quad (82)$$

Throughout, L_i denotes the renormalized low-energy constant/coupling (LEC) at scale μ , and we adopt the convention which is standard in phenomenology, $\mu = M_\rho = 770$ MeV. The normalization used for the decay constants is specified in footnote 2.

5.1.2 Pion form factors and charge radii

The scalar and vector form factors of the pion are defined by the matrix elements

$$\begin{aligned} \langle \pi^i(p_2) | \bar{q} q | \pi^k(p_1) \rangle &= \delta^{ik} F_S^\pi(t), \\ \langle \pi^i(p_2) | \bar{q} \frac{1}{2} \tau^j \gamma^\mu q | \pi^k(p_1) \rangle &= i \epsilon^{ijk} (p_1^\mu + p_2^\mu) F_V^\pi(t), \end{aligned} \quad (83)$$

where the operators contain only the lightest two quark flavours, i.e. τ^1, τ^2, τ^3 are the Pauli matrices, and $t \equiv (p_1 - p_2)^2$ denotes the momentum transfer.

The vector form factor has been measured by several experiments for time-like as well as for space-like values of t . The scalar form factor is not directly measurable, but it can be

evaluated theoretically from data on the $\pi\pi$ and πK phase shifts [15] by means of analyticity and unitarity, i.e. in a model-independent way. Lattice calculations can be compared with data or model-independent theoretical evaluations at any given value of t . At present, however, most lattice studies concentrate on the region close to $t = 0$ and on the evaluation of the slope and curvature which are defined as

$$\begin{aligned} F_V^\pi(t) &= 1 + \frac{1}{6}\langle r^2 \rangle_V^\pi t + c_V t^2 + \dots, \\ F_S^\pi(t) &= F_S^\pi(0) \left[1 + \frac{1}{6}\langle r^2 \rangle_S^\pi t + c_S t^2 + \dots \right]. \end{aligned} \quad (84)$$

The slopes are related to the mean-square vector and scalar radii which are the quantities on which most experiments and lattice calculations concentrate.

In χ PT, the form factors are known at NNLO for $SU(2)$ [16]. The corresponding formulae are available in fully analytical form and are compact enough that they can be used for the chiral extrapolation of the data (as done, for example in Refs. [17, 18]). The expressions for the scalar and vector radii and for the $c_{S,V}$ coefficients at two-loop level read

$$\begin{aligned} \langle r^2 \rangle_S^\pi &= \frac{1}{(4\pi F_\pi)^2} \left\{ 6 \ln \frac{\Lambda_4^2}{M_\pi^2} - \frac{13}{2} - \frac{29}{3} \xi \left(\ln \frac{\Omega_{r_S}^2}{M_\pi^2} \right)^2 + 6\xi k_{r_S} + \mathcal{O}(\xi^2) \right\}, \\ \langle r^2 \rangle_V^\pi &= \frac{1}{(4\pi F_\pi)^2} \left\{ \ln \frac{\Lambda_6^2}{M_\pi^2} - 1 + 2\xi \left(\ln \frac{\Omega_{r_V}^2}{M_\pi^2} \right)^2 + 6\xi k_{r_V} + \mathcal{O}(\xi^2) \right\}, \\ c_S &= \frac{1}{(4\pi F_\pi M_\pi)^2} \left\{ \frac{19}{120} + \xi \left[\frac{43}{36} \left(\ln \frac{\Omega_{c_S}^2}{M_\pi^2} \right)^2 + k_{c_S} \right] \right\}, \\ c_V &= \frac{1}{(4\pi F_\pi M_\pi)^2} \left\{ \frac{1}{60} + \xi \left[\frac{1}{72} \left(\ln \frac{\Omega_{c_V}^2}{M_\pi^2} \right)^2 + k_{c_V} \right] \right\}, \end{aligned} \quad (85)$$

where

$$\begin{aligned} \ln \frac{\Omega_{r_S}^2}{M_\pi^2} &= \frac{1}{29} \left(31 \ln \frac{\Lambda_1^2}{M_\pi^2} + 34 \ln \frac{\Lambda_2^2}{M_\pi^2} - 36 \ln \frac{\Lambda_4^2}{M_\pi^2} + \frac{145}{24} \right), \\ \ln \frac{\Omega_{r_V}^2}{M_\pi^2} &= \frac{1}{2} \left(\ln \frac{\Lambda_1^2}{M_\pi^2} - \ln \frac{\Lambda_2^2}{M_\pi^2} + \ln \frac{\Lambda_4^2}{M_\pi^2} + \ln \frac{\Lambda_6^2}{M_\pi^2} - \frac{31}{12} \right), \\ \ln \frac{\Omega_{c_S}^2}{M_\pi^2} &= \frac{43}{63} \left(11 \ln \frac{\Lambda_1^2}{M_\pi^2} + 14 \ln \frac{\Lambda_2^2}{M_\pi^2} + 18 \ln \frac{\Lambda_4^2}{M_\pi^2} - \frac{6041}{120} \right), \\ \ln \frac{\Omega_{c_V}^2}{M_\pi^2} &= \frac{1}{72} \left(2 \ln \frac{\Lambda_1^2}{M_\pi^2} - 2 \ln \frac{\Lambda_2^2}{M_\pi^2} - \ln \frac{\Lambda_6^2}{M_\pi^2} - \frac{26}{30} \right), \end{aligned} \quad (86)$$

and k_{r_S}, k_{r_V} and k_{c_S}, k_{c_V} are independent of the quark masses. Their expression in terms of the ℓ_i and of the $\mathcal{O}(p^6)$ constants c_M, c_F is known but will not be reproduced here.

The $SU(3)$ formula for the slope of the pion vector form factor reads, to NLO [19],

$$\langle r^2 \rangle_V^\pi \stackrel{\text{NLO}}{=} -\frac{1}{32\pi^2 F_0^2} \left\{ 3 + 2 \ln \frac{M_\pi^2}{\mu^2} + \ln \frac{M_K^2}{\mu^2} \right\} + \frac{12L_9}{F_0^2}, \quad (87)$$

while the expression $\langle r^2 \rangle_S^{\text{oct}}$ for the octet part of the scalar radius does not contain any NLO low-energy constant at one-loop order [19] – contrary to the situation in $SU(2)$, see Eq. (85).

The difference between the quark-line connected and the full (i.e. containing the connected and the disconnected pieces) scalar pion form factor has been investigated by means of χ PT in Ref. [20]. It is expected that the technique used can be applied to a large class of observables relevant in QCD phenomenology.

As a point of practical interest let us remark that there are no finite-volume correction formulae for the mean-square radii $\langle r^2 \rangle_{V,S}$ and the curvatures $c_{V,S}$. The lattice data for $F_{V,S}(t)$ need to be corrected, point by point in t , for finite-volume effects. In fact, if a given t is realized through several inequivalent $p_1 - p_2$ combinations, the level of agreement after the correction has been applied is indicative of how well higher-order effects are under control.

5.1.3 Partially quenched and mixed action formulations

The term “partially quenched QCD” is used in two ways. For heavy quarks (c, b and sometimes s) it usually means that these flavours are included in the valence sector, but not into the functional determinant, i.e. the sea sector. For the light quarks (u, d and sometimes s) it means that they are present in both the valence and the sea sector of the theory, but with different masses (e.g. a series of valence quark masses is evaluated on an ensemble with fixed sea-quark masses).

The program of extending the standard (unitary) $SU(3)$ theory to the (second version of) “partially quenched QCD” has been completed at the two-loop (NNLO) level for masses and decay constants [21]. These formulae tend to be complicated, with the consequence that a state-of-the-art analysis with $\mathcal{O}(2000)$ bootstrap samples on $\mathcal{O}(20)$ ensembles with $\mathcal{O}(5)$ masses each [and hence $\mathcal{O}(200\,000)$ different fits] will require significant computational resources. For a summary of recent developments in χ PT relevant to lattice QCD we refer to Ref. [22]. The $SU(2)$ partially quenched formulae can be obtained from the $SU(3)$ ones by “integrating out the strange quark.” At NLO, they can be found in Ref. [23] by setting the lattice artifact terms from the staggered χ PT form to zero.

The theoretical underpinning of how “partial quenching” is to be understood in the (properly extended) chiral framework is given in Ref. [24]. Specifically, for partially quenched QCD with staggered quarks it is shown that a transfer matrix can be constructed which is not Hermitian but bounded, and can thus be used to construct correlation functions in the usual way. The program of calculating all observables in the p -regime in finite-volume to two loops, first completed in the unitary theory [25, 26], has been carried out for the partially quenched case, too [27].

A further extension of the χ PT framework concerns the lattice effects that arise in partially quenched simulations where sea and valence quarks are implemented with different lattice fermion actions [28–35].

5.1.4 Correlation functions in the ϵ -regime

The finite-size effects encountered in lattice calculations can be used to determine some of the LECs of QCD. In order to illustrate this point, we focus on the two lightest quarks, take the isospin limit $m_u = m_d = m$ and consider a box of size L_s in the three space directions and size L_t in the time direction. If m is sent to zero at fixed box size, chiral symmetry is restored, and the zero-momentum mode of the pion field becomes nonperturbative. An intuitive way to understand the regime with $ML < 1$ ($L = L_s \lesssim L_t$) starts from considering the pion propagator $G(p) = 1/(p^2 + M^2)$ in finite volume. For $ML \gtrsim 1$ and $p \sim 1/L$, $G(p) \sim L^2$ for

small momenta, including $p = 0$. But when M becomes of order $1/L^2$, $G(0) \propto L^4 \gg G(p \neq 0) \sim L^2$. The $p = 0$ mode of the pion field becomes nonperturbative, and the integration over this mode restores chiral symmetry in the limit $m \rightarrow 0$.

The pion effective action for the zero-momentum field depends only on the combination $\mu = m\Sigma V$, the symmetry-restoration parameter, where $V = L_s^3 L_t$. In the ϵ -regime, in which $m \sim 1/V$, all other terms in the effective action are sub-dominant in powers of $\epsilon \sim 1/L$, leading to a reordering of the usual chiral expansion, which assumes that $m \sim \epsilon^2$ instead of $m \sim \epsilon^4$. In the p -regime, with $m \sim \epsilon^2$ or equivalently $ML \gtrsim 1$, finite-volume corrections are of order $\int d^4p e^{ipx} G(p)|_{x \sim L} \sim e^{-ML}$, while in the ϵ -regime, the chiral expansion is an expansion in powers of $1/(\Lambda_{\text{QCD}} L) \sim 1/(FL)$.

As an example, we consider the correlator of the axial charge carried by the two lightest quarks, $q(x) = \{u(x), d(x)\}$. The axial current and the pseudoscalar density are given by

$$A_\mu^i(x) = \bar{q}(x) \frac{1}{2} \tau^i \gamma_\mu \gamma_5 q(x), \quad P^i(x) = \bar{q}(x) \frac{1}{2} \tau^i i \gamma_5 q(x), \quad (88)$$

where τ^1, τ^2, τ^3 are the Pauli matrices in flavour space. In Euclidean space, the correlators of the axial charge and of the space integral over the pseudoscalar density are given by

$$\begin{aligned} \delta^{ik} C_{AA}(t) &= L_s^3 \int d^3\vec{x} \langle A_4^i(\vec{x}, t) A_4^k(0) \rangle, \\ \delta^{ik} C_{PP}(t) &= L_s^3 \int d^3\vec{x} \langle P^i(\vec{x}, t) P^k(0) \rangle. \end{aligned} \quad (89)$$

χ PT yields explicit finite-size scaling formulae for these quantities [12, 36, 37]. In the ϵ -regime, the expansion starts with

$$\begin{aligned} C_{AA}(t) &= \frac{F^2 L_s^3}{L_t} \left[a_A + \frac{L_t}{F^2 L_s^3} b_A h_1\left(\frac{t}{L_t}\right) + \mathcal{O}(\epsilon^4) \right], \\ C_{PP}(t) &= \Sigma^2 L_s^6 \left[a_P + \frac{L_t}{F^2 L_s^3} b_P h_1\left(\frac{t}{L_t}\right) + \mathcal{O}(\epsilon^4) \right], \end{aligned} \quad (90)$$

where the coefficients a_A, b_A, a_P, b_P stand for quantities of $\mathcal{O}(\epsilon^0)$. They can be expressed in terms of the variables L_s, L_t and m and involve only the two leading low-energy constants F and Σ . In fact, at leading order only the combination $\mu = m \Sigma L_s^3 L_t$ matters, the correlators are t -independent and the dependence on μ is fully determined by the structure of the groups involved in the pattern of spontaneous symmetry breaking. In the case of $SU(2) \times SU(2) \rightarrow SU(2)$, relevant for QCD in the symmetry restoration region with two light quarks, the coefficients can be expressed in terms of Bessel functions. The t -dependence of the correlators starts showing up at $\mathcal{O}(\epsilon^2)$, in the form of a parabola, viz. $h_1(\tau) = \frac{1}{2} \left[\left(\tau - \frac{1}{2} \right)^2 - \frac{1}{12} \right]$. Explicit expressions for a_A, b_A, a_P, b_P can be found in Refs. [12, 36, 37], where some of the correlation functions are worked out to NNLO. By matching the finite-size scaling of correlators computed on the lattice with these predictions one can extract F and Σ . A way to deal with the numerical challenges germane to the ϵ -regime has been described [38].

The fact that the representation of the correlators to NLO is not ‘‘contaminated’’ by higher-order unknown LECs, makes the ϵ -regime potentially convenient for a clean extraction of the LO couplings. The determination of these LECs is then affected by different systematic uncertainties with respect to the standard case; simulations in this regime yield complementary information which can serve as a valuable cross-check to get a comprehensive picture of the low-energy properties of QCD.

The effective theory can also be used to study the distribution of the topological charge in QCD [39] and the various quantities of interest may be defined for a fixed value of this charge. The expectation values and correlation functions then not only depend on the symmetry restoration parameter μ , but also on the topological charge ν . The dependence on these two variables can explicitly be calculated. It turns out that the two-point correlation functions considered above retain the form (90), but the coefficients a_A , b_A , a_P , b_P now depend on the topological charge as well as on the symmetry restoration parameter (see Refs. [40–42] for explicit expressions).

A specific issue with ϵ -regime calculations is the scale setting. Ideally one would perform a p -regime study with the same bare parameters to measure a hadronic scale (e.g. the proton mass). In the literature, sometimes a gluonic scale (e.g. r_0) is used to avoid such expenses. Obviously the issues inherent in scale setting are aggravated if the ϵ -regime simulation is restricted to a fixed sector of topological charge.

It is important to stress that in the ϵ -expansion higher-order finite-volume corrections might be significant, and the physical box size (in fm) should still be large in order to keep these distortions under control. The criteria for the chiral extrapolation and finite-volume effects are obviously different with respect to the p -regime. For these reasons we have to adjust the colour coding defined in Sec. 2.1 (see Sec. 5.2 for more details).

Recently, the effective theory has been extended to the “mixed regime” where some quarks are in the p -regime and some in the ϵ -regime [43, 44]. In Ref. [45] a technique is proposed to smoothly connect the p - and ϵ -regimes. In Ref. [46] the issue is reconsidered with a counting rule which is essentially the same as in the p -regime. In this new scheme, one can treat the IR fluctuations of the zero-mode nonperturbatively, while keeping the logarithmic quark mass dependence of the p -regime.

Also first steps towards calculating higher n -point functions in the ϵ -regime have been taken. For instance the electromagnetic pion form factor in QCD has been calculated to NLO in the ϵ -expansion, and a way to get rid of the pion zero-momentum part has been proposed [47].

5.1.5 Energy levels of the QCD Hamiltonian in a box and δ -regime

At low temperature, the properties of the partition function are governed by the lowest eigenvalues of the Hamiltonian. In the case of QCD, the lowest levels are due to the Nambu-Goldstone bosons and can be worked out with χ PT [48]. In the chiral limit the level pattern follows the one of a quantum-mechanical rotator, i.e. $E_\ell = \ell(\ell + 1)/(2\Theta)$ with $\ell = 0, 1, 2, \dots$. For a cubic spatial box and to leading order in the expansion in inverse powers of the box size L_s , the moment of inertia is fixed by the value of the pion decay constant in the chiral limit, i.e. $\Theta = F^2 L_s^3$.

In order to analyse the dependence of the levels on the quark masses and on the parameters that specify the size of the box, a reordering of the chiral series is required, the so-called δ -expansion; the region where the properties of the system are controlled by this expansion is referred to as the δ -regime. Evaluating the chiral series in this regime, one finds that the expansion of the partition function goes in even inverse powers of FL_s , that the rotator formula for the energy levels holds up to NNLO and the expression for the moment of inertia is now also known up to and including terms of order $(FL_s)^{-4}$ [49–51]. Since the level spectrum is governed by the value of the pion decay constant in the chiral limit, an evaluation of this spectrum on the lattice can be used to measure F . More generally, the evaluation of

various observables in the δ -regime offers an alternative method for a determination of some of the low-energy constants occurring in the effective Lagrangian. At present, however, the numerical results obtained in this way [52, 53] are not yet competitive with those found in the p - or ϵ -regime.

5.1.6 Other methods for the extraction of the low-energy constants

An observable that can be used to extract LECs is the topological susceptibility

$$\chi_t = \int d^4x \langle \omega(x)\omega(0) \rangle, \quad (91)$$

where $\omega(x)$ is the topological charge density,

$$\omega(x) = \frac{1}{32\pi^2} \epsilon^{\mu\nu\rho\sigma} \text{Tr} [F_{\mu\nu}(x)F_{\rho\sigma}(x)]. \quad (92)$$

At infinite volume, the expansion of χ_t in powers of the quark masses starts with [54]

$$\chi_t = \bar{m} \Sigma \{1 + \mathcal{O}(m)\}, \quad \bar{m} \equiv \left(\frac{1}{m_u} + \frac{1}{m_d} + \frac{1}{m_s} + \dots \right)^{-1}. \quad (93)$$

The condensate Σ can thus be extracted from the properties of the topological susceptibility close to the chiral limit. The behaviour at finite volume, in particular in the region where the symmetry is restored, is discussed in Ref. [37]. The dependence on the vacuum angle θ and the projection on sectors of fixed ν have been studied in Ref. [39]. For a discussion of the finite-size effects at NLO, including the dependence on θ , we refer to Refs. [42, 55].

The role that the topological susceptibility plays in attempts to determine whether there is a large paramagnetic suppression when going from the $N_f = 2$ to the $N_f = 2 + 1$ theory has been highlighted in Ref. [56]. And the potential usefulness of higher moments of the topological charge distribution to determine LECs has been investigated in Ref. [57].

Another method for computing the quark condensate has been proposed in Ref. [58], where it is shown that starting from the Banks-Casher relation [59] one may extract the condensate from suitable (renormalizable) spectral observables, for instance the number of Dirac operator modes in a given interval. For those spectral observables higher-order corrections can be systematically computed in terms of the chiral effective theory. For recent implementations of this strategy, see Refs. [60–62]. As an aside let us remark that corrections to the Banks-Casher relation that come from a finite quark mass, a finite four-dimensional volume and (with Wilson-type fermions) a finite lattice spacing can be parameterized in a properly extended version of the chiral framework [63, 64].

An alternative strategy is based on the fact that at LO in the ϵ -expansion the partition function in a given topological sector ν is equivalent to the one of a chiral Random Matrix Theory (RMT) [65–68]. In RMT it is possible to extract the probability distributions of individual eigenvalues [69–71] in terms of two dimensionless variables $\zeta = \lambda\Sigma V$ and $\mu = m\Sigma V$, where λ represents the eigenvalue of the massless Dirac operator and m is the sea quark mass. More recently this approach has been extended to the Hermitian (Wilson) Dirac operator [72] which is easier to study in numerical simulations. Hence, if it is possible to match the QCD low-lying spectrum of the Dirac operator to the RMT predictions, then one may extract⁴ the

⁴By introducing an imaginary isospin chemical potential, the framework can be extended such that the low-lying spectrum of the Dirac operator is also sensitive to the pseudoscalar decay constant F at LO [73].

chiral condensate Σ . One issue with this method is that for the distributions of individual eigenvalues higher-order corrections are still not known in the effective theory, and this may introduce systematic effects which are hard⁵ to control. Another open question is that, while it is clear how the spectral density is renormalized [76], this is not the case for the individual eigenvalues, and one relies on assumptions. There have been many lattice studies [77–81] which investigate the matching of the low-lying Dirac spectrum with RMT. In this review the results of the LECs obtained in this way⁶ are not included.

5.2 Extraction of $SU(2)$ low-energy constants

In this and the following subsections we summarize the lattice results for the $SU(2)$ and $SU(3)$ LECs, respectively. In either case we first discuss the $\mathcal{O}(p^2)$ constants and then proceed to their $\mathcal{O}(p^4)$ counterparts. The $\mathcal{O}(p^2)$ LECs are determined from the chiral extrapolation of masses and decay constants or, alternatively, from a finite-size study of correlators in the ϵ -regime. At order p^4 some LECs affect two-point functions while others appear only in three- or four-point functions; the latter need to be determined from form factors or scattering amplitudes. The χ PT analysis of the (nonlattice) phenomenological quantities is nowadays⁷ based on $\mathcal{O}(p^6)$ formulae. At this level the number of LECs explodes and we will not discuss any of these. We will, however, discuss how comparing different orders and different expansions (in particular the x versus ξ -expansion) can help to assess the theoretical uncertainties of the LECs determined on the lattice.

The lattice results for the $SU(2)$ LECs are summarized in Tabs. (19–22) and Figs. (11–13). The tables present our usual colour coding which summarizes the main aspects related to the treatment of the systematic errors of the various calculations.

A delicate issue in the lattice determination of chiral LECs (in particular at NLO) which cannot be reflected by our colour coding is a reliable assessment of the theoretical error that comes from the chiral expansion. We add a few remarks on this point:

1. Using *both* the x and the ξ expansion is a good way to test how the ambiguity of the chiral expansion (at a given order) affects the numerical values of the LECs that are determined from a particular set of data [82, 83]. For instance, to determine $\bar{\ell}_4$ (or Λ_4) from lattice data for F_π as a function of the quark mass, one may compare the fits based on the parameterisation $F_\pi = F\{1 + x \ln(\Lambda_4^2/M^2)\}$ [see Eq. (73)] with those obtained from $F_\pi = F/\{1 - \xi \ln(\Lambda_4^2/M_\pi^2)\}$ [see Eq. (78)]. The difference between the two results provides an estimate of the uncertainty due to the truncation of the chiral series. Which central value one chooses is in principle arbitrary, but we find it advisable to use the one obtained with the ξ expansion,⁸ in particular because it makes the comparison with phenomenological determinations (where it is standard practice to use the ξ expansion) more meaningful.

⁵Higher-order systematic effects in the matching with RMT have been investigated in Refs. [74, 75].

⁶The results for Σ and F lie in the same range as the determinations reported in Tables 19 and 20.

⁷Some of the $\mathcal{O}(p^6)$ formulae presented below have been derived in an unpublished note by three of us (GC, SD and HL) and Jürg Gasser. We thank him for allowing us to publish them here.

⁸There are theoretical arguments suggesting that the ξ expansion is preferable to the x expansion, based on the observation that the coefficients in front of the squared logs in Eq. (73) are somewhat larger than in Eq. (78). This can be traced to the fact that a part of every formula in the x expansion is concerned with locating the position of the pion pole (at the previous order) while in the ξ expansion the knowledge of this position is built in exactly. Numerical evidence supporting this view is presented in Ref. [82].

2. Alternatively one could try to estimate the influence of higher chiral orders by reshuffling irrelevant higher-order terms. For instance, in the example mentioned above one might use $F_\pi = F/\{1 - x \ln(\Lambda_4^2/M^2)\}$ as a different functional form at NLO. Another way to establish such an estimate is through introducing by hand “analytical” higher-order terms (e.g. “analytical NNLO” as done, in the past, by MILC [84]). In principle it would be preferable to include all NNLO terms or none, such that the structure of the chiral expansion is preserved at any order (this is what ETM [85] and JLQCD/TWQCD [82] have done for $SU(2)$ χ PT and MILC for both $SU(2)$ and $SU(3)$ χ PT [86–88]). There are different opinions in the field as to whether it is advisable to include terms to which the data are not sensitive. In case one is willing to include external (typically: nonlattice) information, the use of priors is a theoretically well founded option (e.g. priors for NNLO LECs if one is interested exclusively in LECs at LO/NLO).
3. Another issue concerns the s -quark mass dependence of the LECs $\bar{\ell}_i$ or Λ_i of the $SU(2)$ framework. As far as variations of m_s around m_s^{phys} are concerned (say for $0 < m_s < 1.5m_s^{\text{phys}}$ at best) the issue can be studied in $SU(3)$ χ PT, and this has been done in a series of papers [2, 89, 90]. However, the effect of sending m_s to infinity, as is the case in $N_f = 2$ lattice studies of $SU(2)$ LECs, cannot be addressed in this way. A way to analyse this difference is to compare the numerical values of LECs determined in $N_f = 2$ lattice simulations to those determined in $N_f = 2 + 1$ lattice simulations (see e.g. Ref. [91] for a discussion).
4. Last but not least let us recall that the determination of the LECs is affected by discretisation effects, and it is important that these are removed by means of a continuum extrapolation. In this step invoking an extended version of the chiral Lagrangian [29, 92–96] may be useful⁹ in case one aims for a global fit of lattice data involving several M_π and a values and several chiral observables.

In the tables and figures we summarize the results of various lattice collaborations for the $SU(2)$ LECs at LO (F or F/F_π , B or Σ) and at NLO ($\bar{\ell}_1 - \bar{\ell}_2$, $\bar{\ell}_3$, $\bar{\ell}_4$, $\bar{\ell}_6$). Throughout we group the results into those which stem from $N_f = 2 + 1 + 1$ calculations, those which come from $N_f = 2 + 1$ calculations and those which stem from $N_f = 2$ calculations (since, as mentioned above, the LECs are logically distinct even if the current precision of the data is not sufficient to resolve the differences). Furthermore, we make a distinction whether the results are obtained from simulations in the p -regime or whether alternative methods (ϵ -regime, spectral densities, topological susceptibility, etc.) have been used (this should not affect the result). For comparison we add, in each case, a few representative phenomenological determinations.

A generic comment applies to the issue of the scale setting. In the past none of the lattice studies with $N_f \geq 2$ involved simulations in the p -regime at the physical value of m_{ud} . Accordingly, the setting of the scale a^{-1} via an experimentally measurable quantity did necessarily involve a chiral extrapolation, and as a result of this dimensional quantities used to be particularly sensitive to this extrapolation uncertainty, while in dimensionless ratios such as F_π/F , F/F_0 , B/B_0 , Σ/Σ_0 this particular problem is much reduced (and often finite lattice-to-continuum renormalization factors drop out). Now, there is a new generation of

⁹This means that for any given lattice formulation one needs to determine additional lattice-artifact low-energy constants. For certain formulations, e.g. the twisted-mass approach, first steps in this direction have already been taken [97], while with staggered fermions MILC routinely does so, see e.g. Refs. [84, 98].

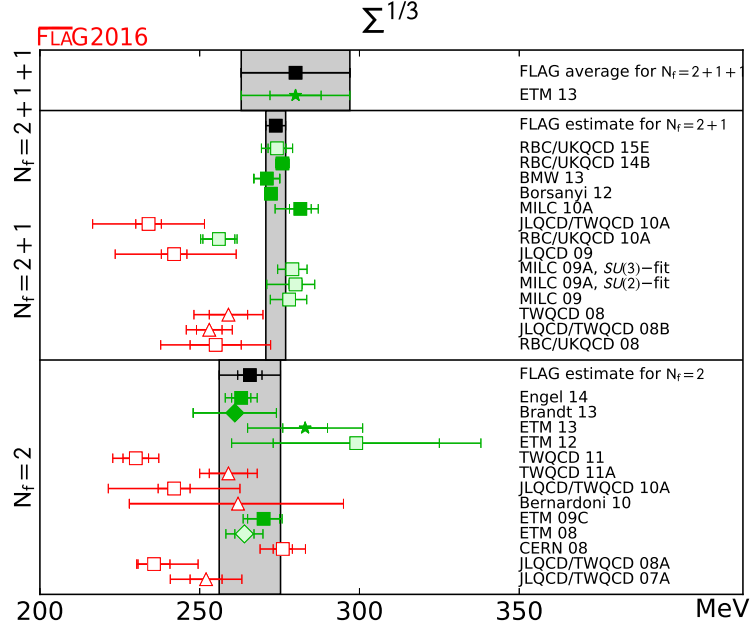


Figure 11: Cubic root of the $SU(2)$ quark condensate $\Sigma \equiv -\langle \bar{u}u \rangle|_{m_u, m_d \rightarrow 0}$ in the $\overline{\text{MS}}$ -scheme, at the renormalization scale $\mu = 2$ GeV. Squares indicate determinations from correlators in the p -regime. Up triangles refer to extractions from the topological susceptibility, diamonds to determinations from the pion form factor, and star symbols refer to the spectral density method.

lattice studies with $N_f = 2$ [99], $N_f = 2 + 1$ [83, 100–108], and $N_f = 2 + 1 + 1$ [109, 110], which does involve simulations at physical pion masses. In such studies the uncertainty that the scale setting has on dimensionful quantities is much mitigated.

It is worth repeating here that the standard colour-coding scheme of our tables is necessarily schematic and cannot do justice to every calculation. In particular there is some difficulty in coming up with a fair adjustment of the rating criteria to finite-volume regimes of QCD. For instance, in the ϵ -regime¹⁰ we re-express the “chiral extrapolation” criterion in terms of $\sqrt{2m_{\min}\Sigma}/F$, with the same threshold values (in MeV) between the three categories as in the p -regime. Also the “infinite volume” assessment is adapted to the ϵ -regime, since the $M_\pi L$ criterion does not make sense here; we assign a green star if at least 2 volumes with $L > 2.5$ fm are included, an open symbol if at least 1 volume with $L > 2$ fm is invoked and a red square if all boxes are smaller than 2 fm. Similarly, in the calculation of form factors and charge radii the tables do not reflect whether an interpolation to the desired q^2 has been performed or whether the relevant q^2 has been engineered by means of “twisted boundary conditions” [113]. In spite of these limitations we feel that these tables give an adequate overview of the qualities of the various calculations.

Collaboration	Ref.	N_f	publication status	chiral extrapolation	continuum extrapolation	finite volume	renormalization	$\Sigma^{1/3}$
ETM 13	[60]	2+1+1	A	○	★	★	★	280(8)(15)
RBC/UKQCD 15E	[108]	2+1	P	★	★	★	★	274.2(2.8)(4.0)
RBC/UKQCD 14B	[107]	2+1	A	★	★	★	★	275.9(1.9)(1.0)
BMW 13	[83]	2+1	A	★	★	★	★	271(4)(1)
Borsanyi 12	[103]	2+1	A	★	★	★	★	272.3(1.2)(1.4)
MILC 10A	[87]	2+1	C	○	★	★	★	281.5(3.4) ^(+2.0) _(-5.9) (4.0)
JLQCD/TWQCD 10A	[112]	2+1	A	★	■	○	★	234(4)(17)
RBC/UKQCD 10A	[114]	2+1	A	○	○	○	★	256(5)(2)(2)
JLQCD 09	[111]	2+1	A	★	■	○	★	242(4) ⁽⁺¹⁹⁾ ₍₋₁₈₎
MILC 09A, $SU(3)$ -fit	[86]	2+1	C	○	★	★	★	279(1)(2)(4)
MILC 09A, $SU(2)$ -fit	[86]	2+1	C	○	★	★	★	280(2) ⁽⁺⁴⁾ ₍₋₈₎ (4)
MILC 09	[84]	2+1	A	○	★	★	★	278(1) ⁽⁺²⁾ ₍₋₃₎ (5)
TWQCD 08	[115]	2+1	A	■	■	■	★	259(6)(9)
JLQCD/TWQCD 08B	[116]	2+1	C	○	■	■	★	249(4)(2)
PACS-CS 08, $SU(3)$ -fit	[117]	2+1	A	★	■	■	■	312(10)
PACS-CS 08, $SU(2)$ -fit	[117]	2+1	A	★	■	■	■	309(7)
RBC/UKQCD 08	[118]	2+1	A	○	■	○	★	255(8)(8)(13)
Engel 14	[62]	2	A	★	★	★	★	263(3)(4)
Brandt 13	[119]	2	A	○	★	○	★	261(13)(1)
ETM 13	[60]	2	A	○	★	○	★	283(7)(17)
ETM 12	[120]	2	A	○	★	○	★	299(26)(29)
Bernardoni 11	[121]	2	C	○	■	■	★	306(11)
TWQCD 11	[122]	2	A	○	■	■	★	230(4)(6)
TWQCD 11A	[123]	2	A	○	■	■	★	259(6)(7)
JLQCD/TWQCD 10A	[112]	2	A	★	■	■	★	242(5)(20)
Bernardoni 10	[124]	2	A	○	■	■	★	262 ⁽⁺³³⁾ ₍₋₃₄₎ ⁽⁺⁴⁾ ₍₋₅₎
ETM 09C	[85]	2	A	○	★	○	★	270(5) ⁽⁺³⁾ ₍₋₄₎
ETM 09B	[125]	2	C	★	■	○	★	245(5)
ETM 08	[17]	2	A	○	○	○	★	264(3)(5)
CERN 08	[58]	2	A	○	■	○	★	276(3)(4)(5)
Hasenfratz 08	[126]	2	A	○	■	★	★	248(6)
JLQCD/TWQCD 08A	[82]	2	A	○	■	■	★	235.7(5.0)(2.0) ^(+12.7) _(-0.0)
JLQCD/TWQCD 07	[127]	2	A	★	■	■	★	239.8(4.0)
JLQCD/TWQCD 07A	[128]	2	A	★	■	■	★	252(5)(10)

Table 19: Cubic root of the $SU(2)$ quark condensate $\Sigma \equiv -\langle \bar{u}u \rangle|_{m_u, m_d \rightarrow 0}$ in MeV units, in the $\overline{\text{MS}}$ -scheme, at the renormalization scale $\mu = 2$ GeV. Horizontal lines separate different N_f . All ETM values which were available only in r_0 units were converted on the basis of $r_0 = 0.48(2)$ fm [99, 129, 130], with this error being added in quadrature to any existing systematic error.

5.2.1 Results for the LO $SU(2)$ LECs

We begin with a discussion of the lattice results for the $SU(2)$ LEC Σ . We present the results in Tab. 19 and Fig. 11. We add that results which include only a statistical error are listed in the table but omitted from the plot. Regarding the $N_f = 2$ computations there are six entries without a red tag. We form the average based on ETM 09C, ETM 13 (here we deviate from our “superseded” rule, since the two works use different methods), Brandt 13, and Engel 14. We add that the last one (with numbers identical to those given in Ref. [61]) is new compared to FLAG 13. Here and in the following we take into account that ETM 09C, ETM 13 share configurations, and the same statement holds true for Brandt 13 and Engel 14. Regarding the $N_f = 2+1$ computations there are four published or updated papers (MILC 10A, Borsanyi 12, BMW 13, and RBC/UKQCD 14B) which qualify for the $N_f = 2+1$ average. The last one is new compared to FLAG 13, and the last but one was not included in the FLAG 13 average, since at the time it was only a preprint.

In slight deviation from the general recipe outlined in Sec. 2.2 we use these values as a basis for our *estimates* (as opposed to *averages*) of the $N_f = 2$ and $N_f = 2+1$ condensates. In each case the central value is obtained from our standard averaging procedure, but the (symmetrical) error is just the median of the overall uncertainties of all contributing results (see the comment below for details). This leads to the values

$$\begin{aligned} N_f = 2 : & \quad \Sigma^{1/3} = 266(10) \text{ MeV} & \quad \text{Refs. [60, 62, 85, 119],} \\ N_f = 2 + 1 : & \quad \Sigma^{1/3} = 274(3) \text{ MeV} & \quad \text{Refs. [83, 87, 103, 107],} \end{aligned} \quad (94)$$

in the $\overline{\text{MS}}$ scheme at the renormalization scale 2 GeV, where the errors include both statistical and systematic uncertainties. In accordance with our guidelines we ask the reader to cite the appropriate set of references as indicated in Eq. (94) when using these numbers. Finally, for $N_f = 2+1+1$ there is only one calculation available, the result of Ref. [60] as given in Tab. 19. According to the conventions of Sec. 2.2 this will be denoted as the “FLAG average” for $N_f = 2+1+1$ in Fig. 11.

As a rationale for using *estimates* (as opposed to *averages*) for $N_f = 2$ and $N_f = 2+1$, we add that for $\Sigma^{1/3}|_{N_f=2}$ and $\Sigma^{1/3}|_{N_f=2+1}$ the standard averaging method would yield central values as quoted in Eq. (94), but with (overall) uncertainties of 4 MeV and 1 MeV, respectively. It is not entirely clear to us that the scale is sufficiently well known in all contributing works to warrant a precision of up to 0.36% on our $\Sigma^{1/3}$, and a similar statement can be made about the level of control over the convergence of the chiral expansion. The aforementioned uncertainties would suggest an N_f -dependence of the $SU(2)$ chiral condensate which (especially in view of similar issues with other LECs, see below) seems premature to us. Therefore we choose to form the central value of our estimate with the standard averaging procedure, but its uncertainty is taken as the median of the uncertainties of the participating results. We hope that future high-quality determinations with both $N_f = 2$, $N_f = 2+1$, and in particular with $N_f = 2+1+1$, will help determine whether there is a noticeable N_f -dependence of the $SU(2)$ chiral condensate or not.

The next quantity considered is F , i.e. the pion decay constant in the $SU(2)$ chiral limit ($m_{ud} \rightarrow 0$, at fixed physical m_s for $N_f > 2$ simulations). As argued on previous occasions we tend to give preference to F_π/F (here the numerator is meant to refer to the physical-pion-mass point) wherever it is available, since often some of the systematic uncertainties are

¹⁰Also in case of Refs. [111, 112] the colour-coding criteria for the ϵ -regime have been applied.

Collaboration	Ref.	N_f	publication status	chiral extrapolation	continuum extrapolation	finite volume	F	F_π/F
ETM 11	[131]	2+1+1	C	○	★	○	85.60(4)	1.077(1)
ETM 10	[132]	2+1+1	A	○	○	★	85.66(6)(13)	1.076(2)(2)
RBC/UKQCD 15E	[108]	2+1	P	★	★	★	85.8(1.1)(1.5)	1.0641(21)(49)
RBC/UKQCD 14B	[107]	2+1	A	★	★	★	86.63(12)(13)	1.0645(15)(0)
BMW 13	[83]	2+1	A	★	★	★	88.0(1.3)(0.3)	1.055(7)(2)
Borsanyi 12	[103]	2+1	A	★	★	★	86.78(05)(25)	1.0627(06)(27)
NPLQCD 11	[133]	2+1	A	○	○	○	86.8(2.1) ^(+3.3) _(-3.4)	1.062(26) ⁽⁺⁴²⁾ ₍₋₄₀₎
MILC 10	[88]	2+1	C	○	★	★	87.0(4)(5)	1.060(5)(6)
MILC 10A	[87]	2+1	C	○	★	★	87.5(1.0) ^(+0.7) _(-2.6)	1.054(12) ⁽⁺³¹⁾ ₍₋₀₉₎
MILC 09A, $SU(3)$ -fit	[86]	2+1	C	○	★	★	86.8(2)(4)	1.062(1)(3)
MILC 09A, $SU(2)$ -fit	[86]	2+1	C	○	★	★	87.4(0.6) ^(+0.9) _(-1.0)	1.054(7) ⁽⁺¹²⁾ ₍₋₁₁₎
MILC 09	[84]	2+1	A	○	★	★	87.66(17) ⁽⁺²⁸⁾ ₍₋₅₂₎	1.052(2) ⁽⁺⁶⁾ ₍₋₃₎
PACS-CS 08, $SU(3)$ -fit	[117]	2+1	A	★	■	■	90.3(3.6)	1.062(8)
PACS-CS 08, $SU(2)$ -fit	[117]	2+1	A	★	■	■	89.4(3.3)	1.060(7)
RBC/UKQCD 08	[118]	2+1	A	○	■	○	81.2(2.9)(5.7)	1.080(8)
ETM 15A	[99]	2	P	★	■	○	86.3(2.8)	1.069(35)
Engel 14	[62]	2	A	★	★	★	85.8(0.7)(2.0)	1.075(09)(25)
Brandt 13	[119]	2	A	○	★	○	84(8)(2)	1.080(16)(6)
QCDSF 13	[134]	2	A	★	○	○	86(1)	1.07(1)
TWQCD 11	[122]	2	A	○	■	■	83.39(35)(38)	1.106(5)(5)
ETM 09C	[85]	2	A	○	★	○	85.91(07) ⁽⁺⁷⁸⁾ ₍₋₀₇₎	1.0755(6) ⁽⁺⁰⁸⁾ ₍₋₉₄₎
ETM 09B	[125]	2	C	★	■	○	92.1(4.9)	1.00(5)
ETM 08	[17]	2	A	○	○	○	86.6(7)(7)	1.067(9)(9)
Hasenfratz 08	[126]	2	A	○	■	★	90(4)	1.02(5)
JLQCD/TWQCD 08A	[82]	2	A	○	■	■	79.0(2.5)(0.7) ^(+4.2) _(-0.0)	1.167(37)(10) ⁽⁺⁰²⁾ ₍₋₆₂₎
JLQCD/TWQCD 07	[127]	2	A	★	■	■	87.3(5.6)	1.06(7)
Colangelo 03	[135]						86.2(5)	1.0719(52)

Table 20: Results for the $SU(2)$ low-energy constant F (in MeV) and for the ratio F_π/F . Horizontal lines separate different N_f . All ETM values which were available only in r_0 units were converted on the basis of $r_0 = 0.48(2)$ fm [99, 129, 130], with this error being added in quadrature to any existing systematic error. Numbers in slanted fonts have been calculated by us, based on $\sqrt{2}F_\pi^{\text{phys}} = 130.41(20)$ MeV [136], with this error being added in quadrature to any existing systematic error.

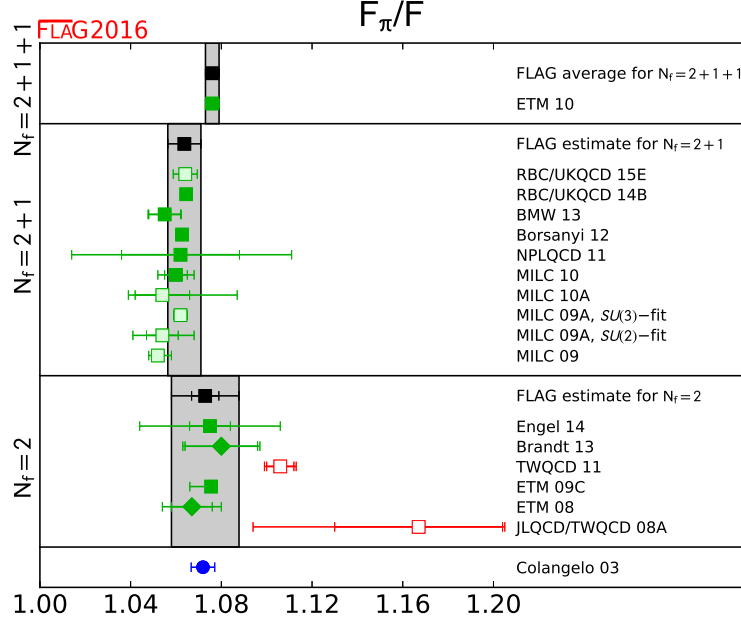


Figure 12: Comparison of the results for the ratio of the physical pion decay constant F_π and the leading-order $SU(2)$ low-energy constant F . The meaning of the symbols is the same as in Fig. 11.

mitigated. We collect the results in Tab. 20 and Fig. 12. In those cases where the collaboration provides only F , the ratio is computed on the basis of the phenomenological value of F_π , and the respective entries in Tab. 20 are in slanted fonts. We encourage authors to provide both F and F_π/F from their analysis, since the ratio is less dependent on the scale setting, and errors tend to partially cancel. Among the $N_f = 2$ determinations five (ETM 08, ETM 09C, QCDSF 13, Brandt 13 and Engel 14) are without red tags. Since the third one is without systematic error, only four of them enter the average. Compared to FLAG 13 the last work is the only one which is new. Among the $N_f = 2 + 1$ determinations five values (MILC 10 as an update of MILC 09, NPLQCD 11, Borsanyi 12, BMW 13, and RBC/UKQCD 14B) contribute to the average. Compared to FLAG 13 the last work is a new addition, and the last but one is included in the average for the first time. Here and in the following we take into account that MILC 10 and NPLQCD 11 share configurations. Finally, there is a single $N_f = 2 + 1 + 1$ determination (ETM 10) which forms the current best estimate in this category.

In analogy to the condensates discussed above, we use these values as a basis for our *estimates* (as opposed to *averages*) of the decay constant ratios

$$\begin{aligned}
 N_f = 2 : & & F_\pi/F &= 1.073(15) & \text{Refs. [17, 62, 85, 119],} \\
 N_f = 2 + 1 : & & F_\pi/F &= 1.064(7) & \text{Refs. [83, 88, 103, 107, 133],}
 \end{aligned} \tag{95}$$

where the errors include both statistical and systematic uncertainties. These numbers are obtained through the well-defined procedure described next to Eq. (94). We ask the reader to cite the appropriate set of references as indicated in Eq. (95) when using these numbers. Finally, for $N_f = 2 + 1 + 1$ the result of Ref. [132] is the only one available; see Tab. 20 for the numerical value.

For this observable the standard averaging method would yield the central values as quoted in Eq. (95), but with (overall) uncertainties of 6 and 1, respectively, on the last digit quoted. In this particular case the single $N_f = 2 + 1 + 1$ determination lies significantly higher than the $N_f = 2 + 1$ *average* (with the small error-bar), basically on par with the $N_f = 2$ *average* (with the small error-bar), and this makes such a standard *average* look even more suspicious to us. At the least, one should wait for one more qualifying $N_f = 2 + 1 + 1$ determination before attempting any conclusions about the N_f dependence of F_π/F . While we are not aware of any theorem which excludes a nonmonotonic behavior in N_f of a LEC, standard physics reasoning would suggest that quark-loop effects become smaller with increasing quark mass, hence a dynamical charm quark will influence LECs less significantly than a dynamical strange quark, and even the latter one seems to bring rather small shifts. As a result, we feel that a nonmonotonic behavior of F_π/F with N_f , once established, would represent a noteworthy finding. We hope this reasoning explains why we prefer to stay in Eq. (95) with *estimates* which obviously are on the conservative side.

5.2.2 Results for the NLO $SU(2)$ LECs

We move on to a discussion of the lattice results for the NLO LECs $\bar{\ell}_3$ and $\bar{\ell}_4$. We remind the reader that on the lattice the former LEC is obtained as a result of the tiny deviation from linearity seen in M_π^2 versus Bm_{ud} , whereas the latter LEC is extracted from the curvature in F_π versus Bm_{ud} . The available determinations are presented in Tab. 21 and Fig. 13. Among the $N_f = 2$ determinations ETM 08, ETM 09C and Brandt 13 are published prior to the deadline, with a systematic uncertainty, and without red tags. Given that the former two use different approaches, all three determinations enter our average. The colour coding of the $N_f = 2 + 1$ results looks very promising; there is a significant number of lattice determinations without any red tag. Applying our superseding rule, MILC 10, NPLQCD 11, Borsanyi 12, BMW 13, and RBC/UKQCD 14B contribute to the average. Compared to the previous edition of our review, the last one is a new addition, and the last but one is included for the first time in the average. For $N_f = 2 + 1 + 1$ there is only the single work ETM 10.

In analogy to our processing of the LECs at LO, we use these determinations as the basis of our *estimate* (as opposed to *average*) of the NLO quantities

$$\begin{aligned} N_f = 2 : & & \bar{\ell}_3 = 3.41(82) & & \text{Refs. [17, 85, 119],} \\ N_f = 2 + 1 : & & \bar{\ell}_3 = 2.81(64) & & \text{Refs. [83, 88, 103, 107, 133],} \end{aligned} \quad (96)$$

$$\begin{aligned} N_f = 2 : & & \bar{\ell}_4 = 4.51(26) & & \text{Refs. [17, 85, 119],} \\ N_f = 2 + 1 : & & \bar{\ell}_4 = 4.10(45) & & \text{Refs. [83, 88, 103, 107, 133],} \end{aligned} \quad (97)$$

where the errors include both statistical and systematic uncertainties. These numbers are obtained through the well-defined procedure described next to Eq. (94). Again we ask the reader to cite the appropriate set of references as indicated in Eq. (96) or Eq. (97) when using these numbers. For $N_f = 2 + 1 + 1$ once again Ref. [132] is the single reference available, see Tab. 21 for the numerical values.

We remark that our preprocessing procedure¹¹ symmetrizes the asymmetric error of ETM 09C with a slight adjustment of the central value. Regarding the difference between the

¹¹There are two naive procedures to symmetrize an asymmetric systematic error: (i) keep the central value untouched and enlarge the smaller error, (ii) shift the central value by half of the difference between the two

Collaboration	Ref.	N_f	publication status	chiral extrapolation	continuum extrapolation	finite volume	$\bar{\ell}_3$	$\bar{\ell}_4$
ETM 11	[131]	2+1+1	C	○	★	○	3.53(5)	4.73(2)
ETM 10	[132]	2+1+1	A	○	○	★	3.70(7)(26)	4.67(3)(10)
RBC/UKQCD 15E	[108]	2+1	P	★	★	★	2.81(19)(45)	4.02(8)(24)
RBC/UKQCD 14B	[107]	2+1	A	★	★	★	2.73(13)(0)	4.113(59)(0)
BMW 13	[83]	2+1	A	★	★	★	2.5(5)(4)	3.8(4)(2)
RBC/UKQCD 12	[106]	2+1	A	★	★	★	2.91(23)(07)	3.99(16)(09)
Borsanyi 12	[103]	2+1	A	★	★	★	3.16(10)(29)	4.03(03)(16)
NPLQCD 11	[133]	2+1	A	○	○	○	4.04(40) ⁽⁺⁷³⁾ ₍₋₅₅₎	4.30(51) ⁽⁺⁸⁴⁾ ₍₋₆₀₎
MILC 10	[88]	2+1	C	○	★	★	3.18(50)(89)	4.29(21)(82)
MILC 10A	[87]	2+1	C	○	★	★	2.85(81) ⁽⁺³⁷⁾ ₍₋₉₂₎	3.98(32) ⁽⁺⁵¹⁾ ₍₋₂₈₎
RBC/UKQCD 10A	[114]	2+1	A	○	○	○	2.57(18)	3.83(9)
MILC 09A, $SU(3)$ -fit	[86]	2+1	C	○	★	★	3.32(64)(45)	4.03(16)(17)
MILC 09A, $SU(2)$ -fit	[86]	2+1	C	○	★	★	3.0(6) ⁽⁺⁹⁾ ₍₋₆₎	3.9(2)(3)
PACS-CS 08, $SU(3)$ -fit	[117]	2+1	A	★	■	■	3.47(11)	4.21(11)
PACS-CS 08, $SU(2)$ -fit	[117]	2+1	A	★	■	■	3.14(23)	4.04(19)
RBC/UKQCD 08	[118]	2+1	A	○	■	○	3.13(33)(24)	4.43(14)(77)
ETM 15A	[99]	2	P	★	■	○		3.3(4)
Gülpers 15	[137]	2	P	★	★	★		4.54(30)(0)
Gülpers 13	[138]	2	A	○	■	○		4.76(13)
Brandt 13	[119]	2	A	○	★	○	3.0(7)(5)	4.7(4)(1)
QCDSF 13	[134]	2	A	★	○	○		4.2(1)
Bernardoni 11	[121]	2	C	○	■	■	4.46(30)(14)	4.56(10)(4)
TWQCD 11	[122]	2	A	○	■	■	4.149(35)(14)	4.582(17)(20)
ETM 09C	[85]	2	A	○	★	○	3.50(9) ⁽⁺⁰⁹⁾ ₍₋₃₀₎	4.66(4) ⁽⁺⁰⁴⁾ ₍₋₃₃₎
JLQCD/TWQCD 09	[139]	2	A	○	■	■		4.09(50)(52)
ETM 08	[17]	2	A	○	○	○	3.2(8)(2)	4.4(2)(1)
JLQCD/TWQCD 08A	[82]	2	A	○	■	■	3.38(40)(24) ⁽⁺³¹⁾ ₍₋₀₀₎	4.12(35)(30) ⁽⁺³¹⁾ ₍₋₀₀₎
CERN-TOV 06	[140]	2	A	○	■	■	3.0(5)(1)	
Colangelo 01	[13]							4.4(2)
Gasser 84	[1]						2.9(2.4)	4.3(9)

Table 21: Results for the $SU(2)$ NLO low-energy constants $\bar{\ell}_3$ and $\bar{\ell}_4$. For comparison, the last two lines show results from phenomenological analyses.

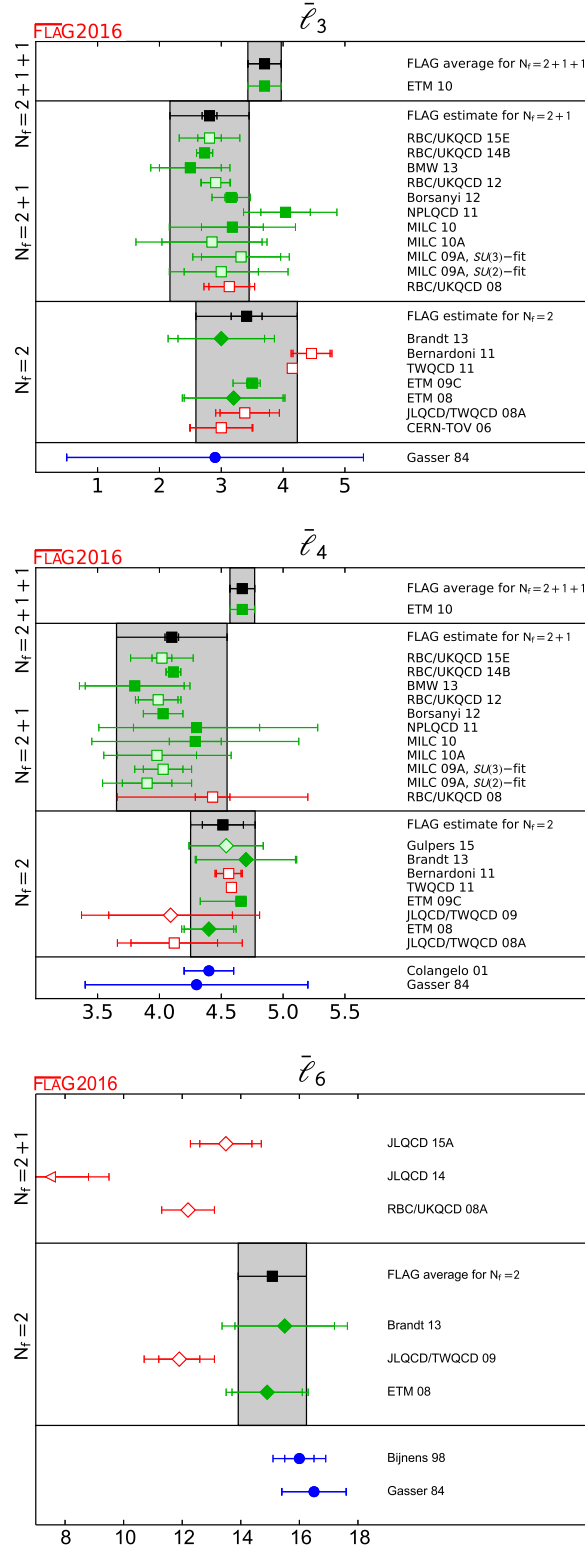


Figure 13: Effective coupling constants $\bar{\ell}_3$, $\bar{\ell}_4$ and $\bar{\ell}_6$. Squares indicate determinations from correlators in the p -regime, diamonds refer to determinations from the pion form factor.

estimates as given in Eqs. (96, 97) and the result of the standard *averaging* procedure we add that the latter would yield the overall uncertainties 25 and 12 for $\bar{\ell}_3$, and the overall uncertainties 17 and 5 for $\bar{\ell}_4$. In all cases the central value would be unchanged. Especially for $\bar{\ell}_4$ such numbers would suggest a clear difference between the value with $N_f = 2$ dynamical flavours and the one at $N_f = 2 + 1$. Similarly to what happened with F_π/F , the single determination with $N_f = 2 + 1 + 1$ is more on the $N_f = 2$ side which, if confirmed, would suggest a nonmonotonicity of a χ P T LEC with N_f . Again we think that currently such a conclusion would be premature, and this is why we give preference to the *estimates* quoted in Eqs. (96, 97).

From a more phenomenological point of view there is a notable difference between $\bar{\ell}_3$ and $\bar{\ell}_4$ in Fig. 13. For $\bar{\ell}_4$ the precision of the phenomenological determination achieved in Colangelo 01 [13] represents a significant improvement compared to Gasser 84 [1]. Picking any N_f , the lattice estimate of $\bar{\ell}_4$ is consistent with both of the phenomenological values and comes with an error-bar which is roughly comparable to or somewhat larger than the one in Colangelo 01 [13]. By contrast, for $\bar{\ell}_3$ the error of an individual lattice computation is usually much smaller than the error of the estimate given in Gasser 84 [1], and even our conservative estimates (96) have uncertainties which represent a significant improvement on the error-bar of Gasser 84 [1]. Evidently, our hope is that future determinations of $\bar{\ell}_3, \bar{\ell}_4$, with $N_f = 2$, $N_f = 2 + 1$ and $N_f = 2 + 1 + 1$, will allow us to further shrink our error-bars in a future edition of FLAG.

We finish with a discussion of the lattice results for $\bar{\ell}_6$ and $\bar{\ell}_1 - \bar{\ell}_2$. The LEC $\bar{\ell}_6$ determines the leading contribution in the chiral expansion of the pion vector charge radius, see Eq. (85). Hence from a lattice study of the vector form factor of the pion with several M_π one may extract the radius $\langle r^2 \rangle_V^\pi$, the curvature c_V (both at the physical pion-mass point) and the LEC $\bar{\ell}_6$ in one go. Similarly, the leading contribution in the chiral expansion of the scalar radius of the pion determines $\bar{\ell}_4$, see Eq. (85). This LEC is also present in the pion-mass dependence of F_π , as we have seen. The difference $\bar{\ell}_1 - \bar{\ell}_2$, finally, may be obtained from the momentum dependence of the vector and scalar pion form factors, based on the two-loop formulae of Ref. [16]. The top part of Tab. 22 collects the results obtained from the vector form factor of the pion (charge radius, curvature and $\bar{\ell}_6$). Regarding this low-energy constant two $N_f = 2$ calculations are published works without a red tag; we thus arrive at the *average* (actually the first one in the LEC section)

$$N_f = 2 : \quad \bar{\ell}_6 = 15.1(1.2) \quad \text{Refs. [17, 119]}, \quad (98)$$

which is represented as a grey band in the last panel of Fig. 13. Here we ask the reader to cite Refs. [17, 119] when using this number.

The experimental information concerning the charge radius is excellent and the curvature is also known very accurately, based on e^+e^- data and dispersion theory. The vector form factor calculations thus present an excellent testing ground for the lattice methodology. The first data column of Tab. 22 shows that most of the available lattice results pass the test. There is, however, one worrisome point. For $\bar{\ell}_6$ the agreement seems less convincing than for the charge radius, even though the two quantities are closely related. In particular the $\bar{\ell}_6$ value of JLQCD 14 [142] seems inconsistent with the phenomenological determinations of

original errors and enlarge/shrink both errors by the same amount. Our procedure (iii) is to average the results of (i) and (ii). In other words a result $c(s) \binom{+u}{-\ell}$ with $\ell > u$ is changed into $c + (u - \ell)/4$ with statistical error s and a symmetric systematic error $(u + 3\ell)/4$. The case $\ell < u$ is handled accordingly.

Collaboration	Ref.	N_f		publication status	chiral extrapolation	continuum extrapolation	finite volume	$\langle r^2 \rangle_V^\pi$	c_V	$\bar{\ell}_6$
HPQCD 15B	[110]	2+1+1	P	★	★	★		0.403(18)(6)		
JLQCD 15A , $SU(2)$ -fit	[141]	2+1	P	○	■	○		0.395(26)(32)		13.49(89)(82)
JLQCD 14	[142]	2+1	A	★	■	■		0.49(4)(4)		7.5(1.3)(1.5)
PACS-CS 11A	[143]	2+1	A	○	■	○		0.441(46)		
RBC/UKQCD 08A	[113]	2+1	A	○	■	○		0.418(31)		12.2(9)
LHP 04	[144]	2+1	A	○	■	■		0.310(46)		
Brandt 13	[119]	2	A	○	★	○		0.481(33)(13)		15.5(1.7)(1.3)
JLQCD/TWQCD 09	[139]	2	A	○	■	■		0.409(23)(37)	3.22(17)(36)	11.9(0.7)(1.0)
ETM 08	[17]	2	A	○	○	○		0.456(30)(24)	3.37(31)(27)	14.9(1.2)(0.7)
QCDSF/UKQCD 06A	[145]	2	A	○	★	○		0.441(19)(63)		
Bijnens 98	[16]							0.437(16)	3.85(60)	16.0(0.5)(0.7)
NA7 86	[146]							0.439(8)		
Gasser 84	[1]									16.5(1.1)

Collaboration	Ref.	N_f		publication status	chiral extrapolation	continuum extrapolation	finite volume	$\langle r^2 \rangle_S^\pi$	$\bar{\ell}_1 - \bar{\ell}_2$
HPQCD 15B	[110]	2+1+1	P	★	★	★		0.481(37)(50)	
RBC/UKQCD 15E	[108]	2+1	P	★	★	★			-9.2(4.9)(6.5)
Gülpers 15	[137]	2	P	★	★	★		0.600(52)(0)	
Gülpers 13	[138]	2	A	○	■	○		0.637(23)	
JLQCD/TWQCD 09	[139]	2	A	○	■	■		0.617(79)(66)	-2.9(0.9)(1.3)
Colangelo 01	[13]							0.61(4)	-4.7(6)

Table 22: Top (vector form factor of the pion): Lattice results for the charge radius $\langle r^2 \rangle_V^\pi$ (in fm^2), the curvature c_V (in GeV^{-4}) and the effective coupling constant $\bar{\ell}_6$ are compared with the experimental value, as obtained by NA7, and some phenomenological estimates. Bottom (scalar form factor of the pion): Lattice results for the scalar radius $\langle r^2 \rangle_S^\pi$ (in fm^2) and the combination $\bar{\ell}_1 - \bar{\ell}_2$ are compared with a dispersive calculation of these quantities.

Refs. [1, 16], even though its value for $\langle r^2 \rangle_V^\pi$ is consistent. So far we have no explanation (other than observing that lattice computations which disagree with the phenomenological determination of $\bar{\ell}_6$ tend to have red tags), but we urge the groups to pay special attention to this point. Similarly, the bottom part of Tab. 22 collects the results obtained for the scalar form factor of the pion and the combination $\bar{\ell}_1 - \bar{\ell}_2$ that is extracted from it. A new feature is that the (yet unpublished) paper [110] gives both the (flavour) octet and singlet part in $SU(3)$, finding $\langle r^2 \rangle_{S,\text{octet}}^\pi = 0.431(38)(46)$ and $\langle r^2 \rangle_{S,\text{singlet}}^\pi = 0.506(38)(53)$. For reasons of backward compatibility they also give $\langle r^2 \rangle_{S,ud}^\pi$ defined with a $\bar{u}u + \bar{d}d$ density, and this number is shown in Tab. 22. Last but not least they find the ordering $\langle r^2 \rangle_{S,\text{conn}}^\pi < \langle r^2 \rangle_{S,\text{octet}}^\pi < \langle r^2 \rangle_{S,ud}^\pi < \langle r^2 \rangle_{S,\text{singlet}}^\pi$ [110].

5.2.3 Epilogue

In this subsection there are several quantities for which only one qualifying (“all-green”) determination is available for a given $SU(2)$ LEC. Obviously the phenomenologically oriented reader is encouraged to use such a value (as provided in our tables) and to cite the original work. We hope that the lattice community will come up with further computations, in particular for $N_f = 2 + 1 + 1$, such that a fair comparison of different works is possible at any N_f , and eventually a statement can be made about the presence or absence of an N_f -dependence of $SU(2)$ LECs.

What can be learned about the convergence pattern of $SU(2)$ χ PT from varying the fit ranges (in m_{ud}) of the pion mass and decay constant (i.e. the quantities from which $\bar{\ell}_3, \bar{\ell}_4$ are derived) is discussed in Ref. [147], where also the usefulness of comparing results from the x and the ξ expansion (with material taken from Ref. [83]) is emphasized.

Perhaps the most important physics result of this subsection is that the lattice simulations confirm the approximate validity of the Gell-Mann-Oakes-Renner formula and show that the square of the pion mass indeed grows in proportion to m_{ud} . The formula represents the leading term of the chiral series and necessarily receives corrections from higher orders. At first nonleading order, the correction is determined by the effective coupling constant $\bar{\ell}_3$. The results collected in Tab. 21 and in the top panel of Fig. 13 show that $\bar{\ell}_3$ is now known quite well. They corroborate the conclusion drawn already in Ref. [148]: the lattice confirms the estimate of $\bar{\ell}_3$ derived in Ref. [1]. In the graph of M_π^2 versus m_{ud} , the values found on the lattice for $\bar{\ell}_3$ correspond to remarkably little curvature: the Gell-Mann-Oakes-Renner formula represents a reasonable first approximation out to values of m_{ud} that exceed the physical value by an order of magnitude.

As emphasized by Stern and collaborators [149–151], the analysis in the framework of χ PT is coherent only if (i) the leading term in the chiral expansion of M_π^2 dominates over the remainder and (ii) the ratio m_s/m_{ud} is close to the value 25.6 that follows from Weinberg’s leading-order formulae. In order to investigate the possibility that one or both of these conditions might fail, the authors proposed a more general framework, referred to as “generalized χ PT”, which includes χ PT as a special case. The results found on the lattice demonstrate that QCD does satisfy both of the above conditions – in the context of QCD, the proposed generalization of the effective theory does not appear to be needed. There is a modified version, however, referred to as “re-summed χ PT” [152], which is motivated by the possibility that the Zweig-rule violating couplings L_4 and L_6 might be larger than expected. The available lattice data do not support this possibility, but they do not rule it out either (see Sec. 5.3 for details).

Collaboration	Ref.	N_f	publication status	chiral extrapolation	continuum extrapolation	finite volume	F_0	F/F_0	B/B_0
JLQCD/TWQCD 10A	[112]	3	A	■	■	■	71(3)(8)		
MILC 10	[88]	2+1	C	○	★	★	80.3(2.5)(5.4)		
MILC 09A	[86]	2+1	C	○	★	★	78.3(1.4)(2.9)	1.104(3)(41)	1.21(4) ⁽⁺⁵⁾ ₍₋₆₎
MILC 09	[84]	2+1	A	○	★	★		1.15(5) ⁽⁺¹³⁾ ₍₋₀₃₎	1.15(16) ⁽⁺³⁹⁾ ₍₋₁₃₎
PACS-CS 08	[117]	2+1	A	★	■	■	83.8(6.4)	1.078(44)	1.089(15)
RBC/UKQCD 08	[118]	2+1	A	○	■	○	66.1(5.2)	1.229(59)	1.03(05)

Collaboration	Ref.	N_f	publication status	chiral extrapolation	continuum extrapolation	finite volume	renormalization	$\Sigma_0^{1/3}$	Σ/Σ_0
JLQCD/TWQCD 10A	[112]	3	A	■	■	■	★	214(6)(24)	1.31(13)(52)
MILC 09A	[86]	2+1	C	○	★	★	★	245(5)(4)(4)	1.48(9)(8)(10)
MILC 09	[84]	2+1	A	○	★	★	★	242(9) ⁽⁺⁰⁵⁾ ₍₋₁₇₎ (4)	1.52(17) ⁽⁺³⁸⁾ ₍₋₁₅₎
PACS-CS 08	[117]	2+1	A	★	■	■	■	290(15)	1.245(10)
RBC/UKQCD 08	[118]	2+1	A	○	■	○	★		1.55(21)

Table 23: Lattice results for the low-energy constants F_0 , B_0 (in MeV) and $\Sigma_0 \equiv F_0^2 B_0$, which specify the effective $SU(3)$ Lagrangian at leading order. The ratios F/F_0 , B/B_0 , Σ/Σ_0 , which compare these with their $SU(2)$ counterparts, indicate the strength of the Zweig-rule violations in these quantities (in the large- N_c limit, they tend to unity). Numbers in slanted fonts are calculated by us, from the information given in the references.

5.3 Extraction of $SU(3)$ low-energy constants

To date, there are three comprehensive $SU(3)$ papers with results based on lattice QCD with $N_f = 2+1$ dynamical flavours [84, 117, 118], and one more with results based on $N_f = 2+1+1$ dynamical flavours [109]. It is an open issue whether the data collected at $m_s \simeq m_s^{\text{phys}}$ allow for an unambiguous determination of $SU(3)$ low-energy constants (cf. the discussion in Ref. [118]). To make definite statements one needs data at considerably smaller m_s , and so far only MILC has some [84]. We are aware of a few papers with a result on one $SU(3)$ low-energy constant each which we list for completeness. Some particulars of the computations are listed in Tab. 23.

Collaboration	Ref.	N_f		publication status	chiral extrapolation	continuum extrapolation	finite volume	$10^3 L_4$	$10^3 L_6$	$10^3(2L_6 - L_4)$
HPQCD 13A	[109]	2+1+1	A	★	★	★		0.09(34)	0.16(20)	0.22(17)
JLQCD/TWQCD 10A	[112]	3	A	■	■	■			0.03(7)(17)	
MILC 10	[88]	2+1	C	○	★	★		-0.08(22) ⁽⁺⁵⁷⁾ ₍₋₃₃₎	-0.02(16) ⁽⁺³³⁾ ₍₋₂₁₎	0.03(24) ⁽⁺³²⁾ ₍₋₂₇₎
MILC 09A	[86]	2+1	C	○	★	★		0.04(13)(4)	0.07(10)(3)	0.10(12)(2)
MILC 09	[84]	2+1	A	○	★	★		0.1(3) ⁽⁺³⁾ ₍₋₁₎	0.2(2) ⁽⁺²⁾ ₍₋₁₎	0.3(1) ⁽⁺²⁾ ₍₋₃₎
PACS-CS 08	[117]	2+1	A	★	■	■		-0.06(10)(-)	0.02(5)(-)	0.10(2)(-)
RBC/UKQCD 08	[118]	2+1	A	○	■	○		0.14(8)(-)	0.07(6)(-)	0.00(4)(-)
Bijnens 11	[22]							0.75(75)	0.29(85)	-0.17(1.86)
Gasser 85	[2]							-0.3(5)	-0.2(3)	-0.1(8)
Collaboration	Ref.	N_f						$10^3 L_5$	$10^3 L_8$	$10^3(2L_8 - L_5)$
HPQCD 13A	[109]	2+1+1	A	★	★	★		1.19(25)	0.55(15)	-0.10(20)
MILC 10	[88]	2+1	C	○	★	★		0.98(16) ⁽⁺²⁸⁾ ₍₋₄₁₎	0.42(10) ⁽⁺²⁷⁾ ₍₋₂₃₎	-0.15(11) ⁽⁺⁴⁵⁾ ₍₋₁₉₎
MILC 09A	[86]	2+1	C	○	★	★		0.84(12)(36)	0.36(5)(7)	-0.12(8)(21)
MILC 09	[84]	2+1	A	○	★	★		1.4(2) ⁽⁺²⁾ ₍₋₁₎	0.8(1)(1)	0.3(1)(1)
PACS-CS 08	[117]	2+1	A	★	■	■		1.45(7)(-)	0.62(4)(-)	-0.21(3)(-)
RBC/UKQCD 08	[118]	2+1	A	○	■	○		0.87(10)(-)	0.56(4)(-)	0.24(4)(-)
NPLQCD 06	[153]	2+1	A	○	■	■		1.42(2) ⁽⁺¹⁸⁾ ₍₋₅₄₎		
Bijnens 11	[22]							0.58(13)	0.18(18)	-0.22(38)
Gasser 85	[2]							1.4(5)	0.9(3)	0.4(8)
Collaboration	Ref.	N_f						$10^3 L_9$	$10^3 L_{10}$	
Boito 15	[154]	2+1	P	★	○	★			-3.50(17)	
JLQCD 15A	[141]	2+1	P	○	■	○		4.6(1.1) ^(+0.1) _(-0.5) (0.4)		
Boyle 14	[155]	2+1	A	★	○	★			-3.46(32)	
JLQCD 14	[142]	2+1	A	★	■	■		2.4(0.8)(1.0)		
RBC/UKQCD 09	[156]	2+1	A	○	■	○			-5.7(11)(07)	
RBC/UKQCD 08A	[113]	2+1	A	○	■	○		3.08(23)(51)		
JLQCD 08A	[157]	2	A	○	■	■			-5.2(2) ⁽⁺⁵⁾ ₍₋₃₎	
Bijnens 02	[158]							5.93(43)		
Davier 98	[159]								-5.13(19)	
Gasser 85	[2]							6.9(7)	-5.5(7)	

Table 24: Low-energy constants of the $SU(3)$ Lagrangian at NLO with running scale $\mu = 770$ MeV (the values in Refs. [2, 84, 86, 88, 109] are evolved accordingly). The MILC 10 entry for L_6 is obtained from their results for $2L_6 - L_4$ and L_4 (similarly for other entries in slanted fonts). The JLQCD 08A result for $\ell_5(770 \text{ MeV})$ [despite the paper saying $L_{10}(770 \text{ MeV})$] was converted to L_{10} with the GL one-loop formula, assuming that the difference between $\bar{\ell}_5(m_s = m_s^{\text{phys}})$ [needed in the formula] and $\bar{\ell}_5(m_s = \infty)$ [computed by JLQCD] is small.

Results for the $SU(3)$ low-energy constants of leading order are found in Tab. 23 and analogous results for some of the effective coupling constants that enter the chiral $SU(3)$ Lagrangian at NLO are collected in Tab. 24. From PACS-CS [117] only those results are quoted which have been *corrected* for finite-size effects (misleadingly labelled “w/FSE” in their tables). For staggered data our colour-coding rule states that M_π is to be understood as M_π^{RMS} . The rating of Refs. [84, 88] is based on the information regarding the RMS masses given in Ref. [86]. Finally, Refs. [154, 155] are “hybrids” in the sense that they combine lattice data and experimental information.

A graphical summary of the lattice results for the coupling constants L_4 , L_5 , L_6 and L_8 , which determine the masses and the decay constants of the pions and kaons at NLO of the chiral $SU(3)$ expansion, is displayed in Fig. 14, along with the two phenomenological determinations quoted in the above tables. The overall consistency seems fairly convincing. In spite of this apparent consistency, there is a point which needs to be clarified as soon as possible. Some collaborations (RBC/UKQCD and PACS-CS) find that they are having difficulties in fitting their partially quenched data to the respective formulas for pion masses above $\simeq 400$ MeV. Evidently, this indicates that the data are stretching the regime of validity of these formulas. To date it is, however, not clear which subset of the data causes the troubles, whether it is the unitary part extending to too large values of the quark masses or whether it is due to $m^{\text{val}}/m^{\text{sea}}$ differing too much from one. In fact, little is known, in the framework of partially quenched χ PT, about the *shape* of the region of applicability in the m^{val} versus m^{sea} plane for fixed N_f . This point has also been emphasized in Ref. [91].

To date only the computations MILC 10 [88] (as an obvious update of MILC 09 and MILC 09A) and HPQCD 13A [109] are free of red tags. Since they use different N_f (in the former case $N_f = 2 + 1$, in the latter case $N_f = 2 + 1 + 1$) we stay away from averaging them. Hence the situation remains unsatisfactory in the sense that for each N_f only a single determination of high standing is available. Accordingly, for the phenomenologically oriented reader there is no alternative to using the results of MILC 10 [88] for $N_f = 2 + 1$ and HPQCD 13A [109] for $N_f = 2 + 1 + 1$, as given in Tab. 24.

5.3.1 Epilogue

In this subsection we find ourselves again in the unpleasant situation that only one qualifying (“all-green”) determination is available (at a given N_f) for several LECs in the $SU(3)$ framework, both at LO and at NLO. Obviously the phenomenologically oriented reader is encouraged to use such a value (as provided in our tables) and to cite the original work. Again our hope is that further computations would become available in forthcoming years, such that a fair comparison of different works will become possible both at $N_f = 2 + 1$ and $N_f = 2 + 1 + 1$.

In the large- N_c limit, the Zweig rule becomes exact, but the quarks have $N_c = 3$. The work done on the lattice is ideally suited to confirm or disprove the approximate validity of this rule for QCD. Two of the coupling constants entering the effective $SU(3)$ Lagrangian at NLO disappear when N_c is sent to infinity: L_4 and L_6 . The upper part of Tab. 24 and the left panels of Fig. 14 show that the lattice results for these quantities are in good agreement. At the scale $\mu = M_\rho$, L_4 and L_6 are consistent with zero, indicating that these constants do approximately obey the Zweig rule. As mentioned above, the ratios F/F_0 , B/B_0 and Σ/Σ_0 also test the validity of this rule. Their expansion in powers of m_s starts with unity and the contributions of first order in m_s are determined by the constants L_4 and L_6 , but they also contain terms of

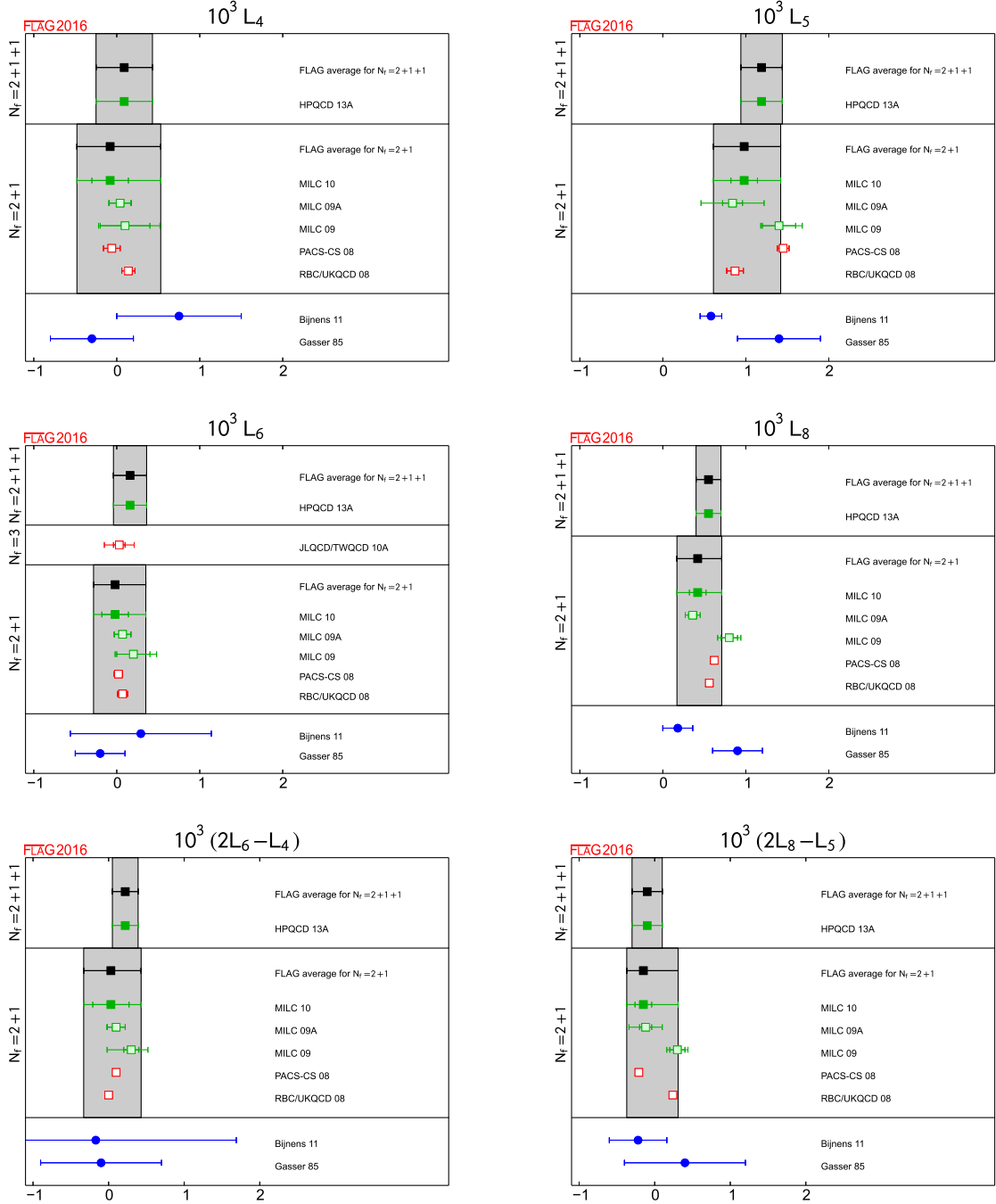


Figure 14: Low-energy constants that enter the effective $SU(3)$ Lagrangian at NLO, with scale $\mu = 770$ MeV. The grey bands labelled as “FLAG average” coincide with the results of MILC 10 [88] for $N_f = 2 + 1$ and with HPQCD 13A [109] for $N_f = 2 + 1 + 1$, respectively.

higher order. Apart from measuring the Zweig-rule violations, an accurate determination of these ratios will thus also allow us to determine the range of m_s where the first few terms of the expansion represent an adequate approximation. Unfortunately, at present, the uncertainties in the lattice data on these ratios are too large to draw conclusions, both concerning the relative size of the subsequent terms in the chiral series and concerning the magnitude of the Zweig-rule violations. The data seem to confirm the *paramagnetic inequalities* [151], which require $F/F_0 > 1$, $\Sigma/\Sigma_0 > 1$, and it appears that the ratio B/B_0 is also larger than unity, but the numerical results need to be improved before further conclusions can be drawn.

The matching formulae in Ref. [2] can be used to calculate the $SU(2)$ couplings \bar{l}_i from the $SU(3)$ couplings L_j . Results obtained in this way are included in Tab. 21, namely the entries explicitly labelled “ $SU(3)$ -fit” as well as MILC 10. Within the still rather large errors, the converted LECs from the $SU(3)$ fits agree with those directly determined within $SU(2)$ χ PT. We plead with every collaboration performing $N_f = 2 + 1$ simulations to also *directly* analyse their data in the $SU(2)$ framework. In practice, lattice simulations are performed at values of m_s close to the physical value and the results are then corrected for the difference of m_s from its physical value. If simulations with more than one value of m_s have been performed, this can be done by interpolation. Alternatively one can use the technique of *re-weighting* (for a review see e.g. Ref. [160]) to shift m_s to its physical value.

References

- [1] J. Gasser and H. Leutwyler, *Chiral perturbation theory to one loop*, *Ann. Phys.* **158** (1984) 142.
- [2] J. Gasser and H. Leutwyler, *Chiral perturbation theory: expansions in the mass of the strange quark*, *Nucl. Phys.* **B250** (1985) 465.
- [3] J. Bijnens and G. Ecker, *Mesonic low-energy constants*, *Ann. Rev. Nucl. Part. Sci.* **64** (2014) 149–174, [[1405.6488](#)].
- [4] S. R. Sharpe, *Applications of chiral perturbation theory to lattice QCD*, Nara, Japan, 2005, [hep-lat/0607016](#).
- [5] M. Golterman, *Applications of chiral perturbation theory to lattice QCD*, in *Modern perspectives in lattice QCD: Quantum field theory and high performance computing. Proceedings, International School, 93rd Session, Les Houches, France, August 3-28, 2009*, pp. 423–515, 2009. [0912.4042](#).
- [6] C. Bernard, *Effective Field Theories and Lattice QCD*, *PoS* **CD15** (2015) 004, [[1510.02180](#)].
- [7] M. E. Fisher and V. Privman, *First-order transitions breaking $O(n)$ symmetry: finite-size scaling*, *Phys. Rev.* **B32** (1985) 447–464.
- [8] E. Brezin and J. Zinn-Justin, *Finite size effects in phase transitions*, *Nucl. Phys.* **B257** (1985) 867.
- [9] J. Gasser and H. Leutwyler, *Light quarks at low temperatures*, *Phys. Lett.* **B184** (1987) 83.
- [10] J. Gasser and H. Leutwyler, *Thermodynamics of chiral symmetry*, *Phys. Lett.* **B188** (1987) 477.
- [11] J. Gasser and H. Leutwyler, *Spontaneously broken symmetries: effective Lagrangians at finite volume*, *Nucl. Phys.* **B307** (1988) 763.
- [12] P. Hasenfratz and H. Leutwyler, *Goldstone boson related finite size effects in field theory and critical phenomena with $O(N)$ symmetry*, *Nucl. Phys.* **B343** (1990) 241–284.
- [13] G. Colangelo, J. Gasser and H. Leutwyler, *$\pi\pi$ scattering*, *Nucl. Phys.* **B603** (2001) 125–179, [[hep-ph/0103088](#)].
- [14] G. Amoros, J. Bijnens and P. Talavera, *Two point functions at two loops in three flavor chiral perturbation theory*, *Nucl. Phys.* **B568** (2000) 319–363, [[hep-ph/9907264](#)].
- [15] J. F. Donoghue, J. Gasser and H. Leutwyler, *The decay of a light Higgs boson*, *Nucl. Phys.* **B343** (1990) 341–368.
- [16] J. Bijnens, G. Colangelo and P. Talavera, *The vector and scalar form factors of the pion to two loops*, *JHEP* **05** (1998) 014, [[hep-ph/9805389](#)].

- [17] [ETM 08] R. Frezzotti, V. Lubicz and S. Simula, *Electromagnetic form factor of the pion from twisted-mass lattice QCD at $N_f = 2$* , *Phys. Rev.* **D79** (2009) 074506, [[0812.4042](#)].
- [18] [JLQCD/TWQCD 08] T. Kaneko et al., *Pion vector and scalar form factors with dynamical overlap quarks*, *PoS LAT2008* (2008) 158, [[0810.2590](#)].
- [19] J. Gasser and H. Leutwyler, *Low-energy expansion of meson form factors*, *Nucl. Phys.* **B250** (1985) 517–538.
- [20] A. Jüttner, *Revisiting the pion’s scalar form factor in chiral perturbation theory*, *JHEP* **1201** (2012) 007, [[1110.4859](#)].
- [21] J. Bijnens, N. Danielsson and T. A. Lähde, *Three-flavor partially quenched chiral perturbation theory at NNLO for meson masses and decay constants*, *Phys. Rev.* **D73** (2006) 074509, [[hep-lat/0602003](#)].
- [22] J. Bijnens and I. Jemos, *A new global fit of the L_i^T at next-to-next-to-leading order in chiral perturbation theory*, *Nucl.Phys.* **B854** (2012) 631–665, [[1103.5945](#)].
- [23] X. Du, *Staggered chiral perturbation theory in the two-flavor case*, *Phys. Rev.* **D82** (2010) 014016, [[0911.2534](#)].
- [24] C. Bernard and M. Golterman, *On the foundations of partially quenched chiral perturbation theory*, *Phys.Rev.* **D88** (2013) 014004, [[1304.1948](#)].
- [25] J. Bijnens, E. Bostrom and T. A. Lahde, *Two-loop sunset integrals at finite volume*, *JHEP* **01** (2014) 019, [[1311.3531](#)].
- [26] J. Bijnens and T. Rössler, *Finite volume at two-loops in chiral perturbation theory*, *JHEP* **01** (2015) 034, [[1411.6384](#)].
- [27] J. Bijnens and T. Rössler, *Finite Volume for Three-Flavour Partially Quenched Chiral Perturbation Theory through NNLO in the Meson Sector*, *JHEP* **11** (2015) 097, [[1508.07238](#)].
- [28] O. Bär, G. Rupak and N. Shoresh, *Simulations with different lattice Dirac operators for valence and sea quarks*, *Phys. Rev.* **D67** (2003) 114505, [[hep-lat/0210050](#)].
- [29] O. Bär, G. Rupak and N. Shoresh, *Chiral perturbation theory at $O(a^2)$ for lattice QCD*, *Phys. Rev.* **D70** (2004) 034508, [[hep-lat/0306021](#)].
- [30] O. Bär, C. Bernard, G. Rupak and N. Shoresh, *Chiral perturbation theory for staggered sea quarks and Ginsparg-Wilson valence quarks*, *Phys. Rev.* **D72** (2005) 054502, [[hep-lat/0503009](#)].
- [31] J.-W. Chen, M. Golterman, D. O’Connell and A. Walker-Loud, *Mixed action effective field theory: an addendum*, *Phys. Rev.* **D79** (2009) 117502, [[0905.2566](#)].
- [32] [SWME 10] T. Bae et al., *B_K using HYP-smearred staggered fermions in $N_f = 2 + 1$ unquenched QCD*, *Phys. Rev.* **D82** (2010) 114509, [[1008.5179](#)].

- [33] J. A. Bailey, H.-J. Kim, W. Lee and S. R. Sharpe, *Kaon mixing matrix elements from beyond-the-Standard-Model operators in staggered chiral perturbation theory*, *Phys. Rev.* **D85** (2012) 074507, [[1202.1570](#)].
- [34] C. Bernard, J. Bijnens and E. Gamiz, *Semileptonic kaon decay in staggered chiral perturbation theory*, *Phys. Rev.* **D89** (2014) 054510, [[1311.7511](#)].
- [35] [SWME 15] J.A. Bailey, H.-J. Kim, J. Kim, W. Lee and B. Yoon, *Masses and decay constants of pions and kaons in mixed-action staggered chiral perturbation theory*, [1504.02573](#).
- [36] F. C. Hansen, *Finite size effects in spontaneously broken $SU(N)\times SU(N)$ theories*, *Nucl. Phys.* **B345** (1990) 685–708.
- [37] F. C. Hansen and H. Leutwyler, *Charge correlations and topological susceptibility in QCD*, *Nucl. Phys.* **B350** (1991) 201–227.
- [38] L. Giusti, P. Hernandez, M. Laine, P. Weisz and H. Wittig, *Low-energy couplings of QCD from current correlators near the chiral limit*, *JHEP* **0404** (2004) 013, [[hep-lat/0402002](#)].
- [39] H. Leutwyler and A. V. Smilga, *Spectrum of Dirac operator and role of winding number in QCD*, *Phys. Rev.* **D46** (1992) 5607–5632.
- [40] P. H. Damgaard, M. C. Diamantini, P. Hernandez and K. Jansen, *Finite-size scaling of meson propagators*, *Nucl. Phys.* **B629** (2002) 445–478, [[hep-lat/0112016](#)].
- [41] P. H. Damgaard, P. Hernandez, K. Jansen, M. Laine and L. Lellouch, *Finite-size scaling of vector and axial current correlators*, *Nucl. Phys.* **B656** (2003) 226–238, [[hep-lat/0211020](#)].
- [42] S. Aoki and H. Fukaya, *Chiral perturbation theory in a θ vacuum*, *Phys. Rev.* **D81** (2010) 034022, [[0906.4852](#)].
- [43] F. Bernardoni, P. H. Damgaard, H. Fukaya and P. Hernandez, *Finite volume scaling of Pseudo Nambu-Goldstone Bosons in QCD*, *JHEP* **10** (2008) 008, [[0808.1986](#)].
- [44] P. Hernandez, S. Necco, C. Pena and G. Vulvert, *$N_f = 2$ chiral dynamics in the mixed chiral regime*, *PoS LAT2012* (2012) 204, [[1211.1488](#)].
- [45] P. H. Damgaard and H. Fukaya, *The chiral condensate in a finite volume*, *JHEP* **01** (2009) 052, [[0812.2797](#)].
- [46] S. Aoki and H. Fukaya, *Interpolation between the ϵ - and p -regimes*, *Phys.Rev.* **D84** (2011) 014501, [[1105.1606](#)].
- [47] H. Fukaya and T. Suzuki, *Extracting the electromagnetic pion form factor from QCD in a finite volume*, *Phys. Rev.* **D90** (2014) 114508, [[1409.0327](#)].
- [48] H. Leutwyler, *Energy levels of light quarks confined to a box*, *Phys. Lett.* **B189** (1987) 197.

- [49] P. Hasenfratz, *The QCD rotator in the chiral limit*, *Nucl. Phys.* **B828** (2010) 201–214, [[0909.3419](#)].
- [50] F. Niedermayer and C. Weiermann, *The rotator spectrum in the δ -regime of the $O(n)$ effective field theory in 3 and 4 dimensions*, *Nucl. Phys.* **B842** (2011) 248–263, [[1006.5855](#)].
- [51] M. Weingart, *The QCD rotator with a light quark mass*, [1006.5076](#).
- [52] A. Hasenfratz, P. Hasenfratz, F. Niedermayer, D. Hierl and A. Schäfer, *First results in QCD with 2+1 light flavors using the fixed-point action*, *PoS LAT2006* (2006) 178, [[hep-lat/0610096](#)].
- [53] [QCDSF 10] W. Bietenholz et al., *Pion in a box*, *Phys. Lett.* **B687** (2010) 410–414, [[1002.1696](#)].
- [54] P. Di Vecchia and G. Veneziano, *Chiral dynamics in the large N limit*, *Nucl. Phys.* **B171** (1980) 253.
- [55] [TWQCD 09] Y.-Y. Mao and T.-W. Chiu, *Topological susceptibility to the one-loop order in chiral perturbation theory*, *Phys. Rev.* **D80** (2009) 034502, [[0903.2146](#)].
- [56] V. Bernard, S. Descotes-Genon and G. Toucas, *Topological susceptibility on the lattice and the three-flavour quark condensate*, *JHEP* **1206** (2012) 051, [[1203.0508](#)].
- [57] V. Bernard, S. Descotes-Genon and G. Toucas, *Determining the chiral condensate from the distribution of the winding number beyond topological susceptibility*, *JHEP* **12** (2012) 080, [[1209.4367](#)].
- [58] [CERN 08] L. Giusti and M. Lüscher, *Chiral symmetry breaking and the Banks–Casher relation in lattice QCD with Wilson quarks*, *JHEP* **03** (2009) 013, [[0812.3638](#)].
- [59] T. Banks and A. Casher, *Chiral symmetry breaking in confining theories*, *Nucl. Phys.* **B169** (1980) 103.
- [60] [ETM 13] K. Cichy, E. Garcia-Ramos and K. Jansen, *Chiral condensate from the twisted mass Dirac operator spectrum*, *JHEP* **1310** (2013) 175, [[1303.1954](#)].
- [61] G. P. Engel, L. Giusti, S. Lottini and R. Sommer, *Chiral Symmetry Breaking in QCD with Two Light Flavors*, *Phys. Rev. Lett.* **114** (2015) 112001, [[1406.4987](#)].
- [62] G. P. Engel, L. Giusti, S. Lottini and R. Sommer, *Spectral density of the Dirac operator in two-flavor QCD*, *Phys. Rev.* **D91** (2015) 054505, [[1411.6386](#)].
- [63] S. R. Sharpe, *Discretization errors in the spectrum of the Hermitian Wilson-Dirac operator*, *Phys. Rev.* **D74** (2006) 014512, [[hep-lat/0606002](#)].
- [64] S. Necco and A. Shindler, *Corrections to the Banks-Casher relation with Wilson quarks*, *PoS CD12* (2012) 056, [[1302.5595](#)].
- [65] E. V. Shuryak and J. J. M. Verbaarschot, *Random matrix theory and spectral sum rules for the Dirac operator in QCD*, *Nucl. Phys.* **A560** (1993) 306–320, [[hep-th/9212088](#)].

- [66] J. J. M. Verbaarschot and I. Zahed, *Spectral density of the QCD Dirac operator near zero virtuality*, *Phys. Rev. Lett.* **70** (1993) 3852–3855, [[hep-th/9303012](#)].
- [67] J. J. M. Verbaarschot, *The spectrum of the QCD Dirac operator and chiral random matrix theory: the threefold way*, *Phys. Rev. Lett.* **72** (1994) 2531–2533, [[hep-th/9401059](#)].
- [68] J. J. M. Verbaarschot and T. Wettig, *Random matrix theory and chiral symmetry in QCD*, *Ann. Rev. Nucl. Part. Sci.* **50** (2000) 343–410, [[hep-ph/0003017](#)].
- [69] S. M. Nishigaki, P. H. Damgaard and T. Wettig, *Smallest Dirac eigenvalue distribution from random matrix theory*, *Phys. Rev.* **D58** (1998) 087704, [[hep-th/9803007](#)].
- [70] P. H. Damgaard and S. M. Nishigaki, *Distribution of the k -th smallest Dirac operator eigenvalue*, *Phys. Rev.* **D63** (2001) 045012, [[hep-th/0006111](#)].
- [71] F. Basile and G. Akemann, *Equivalence of QCD in the ϵ -regime and chiral random matrix theory with or without chemical potential*, *JHEP* **12** (2007) 043, [[0710.0376](#)].
- [72] M. Kieburg, J. J. M. Verbaarschot and S. Zafeiropoulos, *Random matrix models for the hermitian Wilson-Dirac operator of QCD-like theories*, *PoS LAT2012* (2012) 209, [[1303.3242](#)].
- [73] G. Akemann, P. H. Damgaard, J. C. Osborn and K. Splittorff, *A new chiral two-matrix theory for Dirac spectra with imaginary chemical potential*, *Nucl. Phys.* **B766** (2007) 34–67, [[hep-th/0609059](#)].
- [74] C. Lehner, S. Hashimoto and T. Wettig, *The ϵ -expansion at next-to-next-to-leading order with small imaginary chemical potential*, *JHEP* **06** (2010) 028, [[1004.5584](#)].
- [75] C. Lehner, J. Bloch, S. Hashimoto and T. Wettig, *Geometry dependence of RMT-based methods to extract the low-energy constants Σ and F* , *JHEP* **1105** (2011) 115, [[1101.5576](#)].
- [76] [CERN-TOV 05] L. Del Debbio, L. Giusti, M. Lüscher, R. Petronzio and N. Tantalo, *Stability of lattice QCD simulations and the thermodynamic limit*, *JHEP* **02** (2006) 011, [[hep-lat/0512021](#)].
- [77] [JLQCD/TWQCD 07B] H. Fukaya et al., *Two-flavor lattice QCD in the ϵ -regime and chiral random matrix theory*, *Phys. Rev.* **D76** (2007) 054503, [[0705.3322](#)].
- [78] [BGR 06] C. B. Lang, P. Majumdar and W. Ortner, *The condensate for two dynamical chirally improved quarks in QCD*, *Phys. Lett.* **B649** (2007) 225–229, [[hep-lat/0611010](#)].
- [79] T. DeGrand, Z. Liu and S. Schaefer, *Quark condensate in two-flavor QCD*, *Phys. Rev.* **D74** (2006) 094504, [[hep-lat/0608019](#)].
- [80] P. Hasenfratz et al., *2+1 flavor QCD simulated in the ϵ -regime in different topological sectors*, *JHEP* **11** (2009) 100, [[0707.0071](#)].
- [81] T. DeGrand and S. Schaefer, *Parameters of the lowest order chiral Lagrangian from fermion eigenvalues*, *Phys. Rev.* **D76** (2007) 094509, [[0708.1731](#)].

- [82] [JLQCD/TWQCD 08A] J. Noaki et al., *Convergence of the chiral expansion in two-flavor lattice QCD*, *Phys. Rev. Lett.* **101** (2008) 202004, [[0806.0894](#)].
- [83] [BMW 13] S. Dürer, Z. Fodor, C. Hoelbling, S. Krieg, T. Kurth et al., *Lattice QCD at the physical point meets $SU(2)$ chiral perturbation theory*, *Phys. Rev.* **D90** (2014) 114504, [[1310.3626](#)].
- [84] [MILC 09] A. Bazavov et al., *Full nonperturbative QCD simulations with 2+1 flavors of improved staggered quarks*, *Rev. Mod. Phys.* **82** (2010) 1349–1417, [[0903.3598](#)].
- [85] [ETM 09C] R. Baron et al., *Light meson physics from maximally twisted mass lattice QCD*, *JHEP* **08** (2010) 097, [[0911.5061](#)].
- [86] [MILC 09A] A. Bazavov et al., *MILC results for light pseudoscalars*, *PoS* **CD09** (2009) 007, [[0910.2966](#)].
- [87] [MILC 10A] A. Bazavov et al., *Staggered chiral perturbation theory in the two-flavor case and $SU(2)$ analysis of the MILC data*, *PoS* **LAT2010** (2010) 083, [[1011.1792](#)].
- [88] [MILC 10] A. Bazavov et al., *Results for light pseudoscalar mesons*, *PoS* **LAT2010** (2010) 074, [[1012.0868](#)].
- [89] J. Gasser, C. Haefeli, M. A. Ivanov and M. Schmid, *Integrating out strange quarks in ChPT*, *Phys. Lett.* **B652** (2007) 21–26, [[0706.0955](#)].
- [90] J. Gasser, C. Haefeli, M. A. Ivanov and M. Schmid, *Integrating out strange quarks in ChPT: terms at order p^6* , *Phys. Lett.* **B675** (2009) 49–53, [[0903.0801](#)].
- [91] S. Dürer, *Convergence issues in ChPT: a lattice perspective*, *PoS* **KAON13** (2013) 027, [[1305.5758](#)].
- [92] G. Rupak and N. Shoresh, *Chiral perturbation theory for the Wilson lattice action*, *Phys. Rev.* **D66** (2002) 054503, [[hep-lat/0201019](#)].
- [93] S. Aoki, *Chiral perturbation theory with Wilson-type fermions including a^2 effects: $N_f = 2$ degenerate case*, *Phys. Rev.* **D68** (2003) 054508, [[hep-lat/0306027](#)].
- [94] C. Aubin and C. Bernard, *Pion and kaon masses in staggered chiral perturbation theory*, *Phys. Rev.* **D68** (2003) 034014, [[hep-lat/0304014](#)].
- [95] C. Aubin and C. Bernard, *Pseudoscalar decay constants in staggered chiral perturbation theory*, *Phys. Rev.* **D68** (2003) 074011, [[hep-lat/0306026](#)].
- [96] O. Bär and B. Horz, *Charmless chiral perturbation theory for $N_f = 2 + 1 + 1$ twisted mass lattice QCD*, *Phys. Rev.* **D90** (2014) 034508, [[1402.6145](#)].
- [97] [ETM 13A] G. Herdoiza, K. Jansen, C. Michael, K. Ottnad and C. Urbach, *Determination of low-energy constants of Wilson chiral perturbation theory*, *JHEP* **1305** (2013) 038, [[1303.3516](#)].
- [98] [MILC 04] C. Aubin et al., *Light pseudoscalar decay constants, quark masses and low energy constants from three-flavor lattice QCD*, *Phys. Rev.* **D70** (2004) 114501, [[hep-lat/0407028](#)].

- [99] [ETM 15A] A. Abdel-Rehim et al., *Simulating QCD at the physical point with $N_f = 2$ Wilson twisted mass fermions at maximal twist*, [1507.05068](#).
- [100] [PACS-CS 09] S. Aoki et al., *Physical point simulation in 2+1 flavor lattice QCD*, *Phys. Rev.* **D81** (2010) 074503, [[0911.2561](#)].
- [101] [BMW 10A] S. Dürer, Z. Fodor, C. Hoelbling, S. Katz, S. Krieg et al., *Lattice QCD at the physical point: light quark masses*, *Phys.Lett.* **B701** (2011) 265–268, [[1011.2403](#)].
- [102] [BMW 10B] S. Dürer, Z. Fodor, C. Hoelbling, S. Katz, S. Krieg et al., *Lattice QCD at the physical point: simulation and analysis details*, *JHEP* **1108** (2011) 148, [[1011.2711](#)].
- [103] S. Borsanyi, S. Dürer, Z. Fodor, S. Krieg, A. Schäfer et al., *SU(2) chiral perturbation theory low-energy constants from 2+1 flavor staggered lattice simulations*, *Phys.Rev.* **D88** (2013) 014513, [[1205.0788](#)].
- [104] [MILC 12B] A. Bazavov et al., *Lattice QCD ensembles with four flavors of highly improved staggered quarks*, *Phys.Rev.* **D87** (2013) 054505, [[1212.4768](#)].
- [105] [FNAL/MILC 12I] A. Bazavov, C. Bernard, C. Bouchard, C. DeTar, D. Du et al., *Kaon semileptonic vector form factor and determination of $|V_{us}|$ using staggered fermions*, *Phys.Rev.* **D87** (2013) 073012, [[1212.4993](#)].
- [106] [RBC/UKQCD 12] R. Arthur et al., *Domain wall QCD with near-physical pions*, *Phys.Rev.* **D87** (2013) 094514, [[1208.4412](#)].
- [107] [RBC/UKQCD 14B] T. Blum et al., *Domain wall QCD with physical quark masses*, *Phys. Rev.* **D93** (2016) 074505, [[1411.7017](#)].
- [108] [RBC/UKQCD 15E] P. A. Boyle et al., *Low energy constants of SU(2) partially quenched chiral perturbation theory from $N_f=2+1$ domain wall QCD*, *Phys. Rev.* **D93** (2016) 054502, [[1511.01950](#)].
- [109] [HPQCD 13A] R. Dowdall, C. Davies, G. Lepage and C. McNeile, *V_{us} from π and K decay constants in full lattice QCD with physical u , d , s and c quarks*, *Phys.Rev.* **D88** (2013) 074504, [[1303.1670](#)].
- [110] [HPQCD 15B] J. Koponen, F. Bursa, C. T. H. Davies, R. J. Dowdall and G. P. Lepage, *The Size of the Pion from Full Lattice QCD with Physical u , d , s and c Quarks*, *Phys. Rev.* **D93** (2016) 054503, [[1511.07382](#)].
- [111] [JLQCD 09] H. Fukaya et al., *Determination of the chiral condensate from 2+1-flavor lattice QCD*, *Phys. Rev. Lett.* **104** (2010) 122002, [[0911.5555](#)].
- [112] [JLQCD/TWQCD 10A] H. Fukaya et al., *Determination of the chiral condensate from QCD Dirac spectrum on the lattice*, *Phys. Rev.* **D83** (2011) 074501, [[1012.4052](#)].
- [113] [RBC/UKQCD 08A] P. A. Boyle et al., *The pion's electromagnetic form factor at small momentum transfer in full lattice QCD*, *JHEP* **07** (2008) 112, [[0804.3971](#)].
- [114] [RBC/UKQCD 10A] Y. Aoki et al., *Continuum limit physics from 2+1 flavor domain wall QCD*, *Phys.Rev.* **D83** (2011) 074508, [[1011.0892](#)].

- [115] [TWQCD 08] T.-W. Chiu, T.-H. Hsieh and P.-K. Tseng, *Topological susceptibility in 2+1 flavors lattice QCD with domain-wall fermions*, *Phys. Lett.* **B671** (2009) 135–138, [[0810.3406](#)].
- [116] [JLQCD/TWQCD 08B] T.-W. Chiu et al., *Topological susceptibility in (2+1)-flavor lattice QCD with overlap fermion*, *PoS LAT2008* (2008) 072, [[0810.0085](#)].
- [117] [PACS-CS 08] S. Aoki et al., *2+1 flavor lattice QCD toward the physical point*, *Phys. Rev.* **D79** (2009) 034503, [[0807.1661](#)].
- [118] [RBC/UKQCD 08] C. Allton et al., *Physical results from 2+1 flavor domain wall QCD and $SU(2)$ chiral perturbation theory*, *Phys. Rev.* **D78** (2008) 114509, [[0804.0473](#)].
- [119] B. B. Brandt, A. Jüttner and H. Wittig, *The pion vector form factor from lattice QCD and NNLO chiral perturbation theory*, *JHEP* **1311** (2013) 034, [[1306.2916](#)].
- [120] [ETM 12] F. Burger, V. Lubicz, M. Muller-Preussker, S. Simula and C. Urbach, *Quark mass and chiral condensate from the Wilson twisted mass lattice quark propagator*, *Phys.Rev.* **D87** (2013) 034514, [[1210.0838](#)].
- [121] F. Bernardoni, N. Garron, P. Hernandez, S. Necco and C. Pena, *Light quark correlators in a mixed-action setup*, *PoS LAT2011* (2011) 109, [[1110.0922](#)].
- [122] [TWQCD 11] T.-W. Chiu, T.-H. Hsieh and Y.-Y. Mao, *Pseudoscalar meson in two flavors QCD with the optimal domain-wall fermion*, *Phys.Lett.* **B717** (2012) 420–424, [[1109.3675](#)].
- [123] [TWQCD 11A] T.-W. Chiu, T. H. Hsieh and Y. Y. Mao, *Topological susceptibility in two flavors lattice QCD with the optimal domain-wall fermion*, *Phys.Lett.* **B702** (2011) 131–134, [[1105.4414](#)].
- [124] F. Bernardoni, P. Hernandez, N. Garron, S. Necco and C. Pena, *Probing the chiral regime of $N_f = 2$ QCD with mixed actions*, *Phys. Rev.* **D83** (2011) 054503, [[1008.1870](#)].
- [125] [ETM 09B] K. Jansen and A. Shindler, *The ϵ -regime of chiral perturbation theory with Wilson-type fermions*, *PoS LAT2009* (2009) 070, [[0911.1931](#)].
- [126] A. Hasenfratz, R. Hoffmann and S. Schaefer, *Low energy chiral constants from ϵ -regime simulations with improved Wilson fermions*, *Phys. Rev.* **D78** (2008) 054511, [[0806.4586](#)].
- [127] [JLQCD/TWQCD 07] H. Fukaya et al., *Lattice study of meson correlators in the ϵ -regime of two-flavor QCD*, *Phys. Rev.* **D77** (2008) 074503, [[0711.4965](#)].
- [128] [JLQCD/TWQCD 07A] S. Aoki et al., *Topological susceptibility in two-flavor lattice QCD with exact chiral symmetry*, *Phys. Lett.* **B665** (2008) 294–297, [[0710.1130](#)].
- [129] Y. Aoki, S. Borsanyi, S. Durr, Z. Fodor, S. D. Katz, S. Krieg et al., *The QCD transition temperature: results with physical masses in the continuum limit II.*, *JHEP* **06** (2009) 088, [[0903.4155](#)].

- [130] [HotQCD 14] A. Bazavov et al., *Equation of state in (2+1)-flavor QCD*, *Phys.Rev.* **D90** (2014) 094503, [[1407.6387](#)].
- [131] [ETM 11] R. Baron et al., *Light hadrons from $N_f = 2 + 1 + 1$ dynamical twisted mass fermions*, *PoS LAT2010* (2010) 123, [[1101.0518](#)].
- [132] [ETM 10] R. Baron et al., *Light hadrons from lattice QCD with light (u,d), strange and charm dynamical quarks*, *JHEP* **1006** (2010) 111, [[1004.5284](#)].
- [133] [NPLQCD 11] S. R. Beane, W. Detmold, P. Junnarkar, T. Luu, K. Orginos et al., *$SU(2)$ low-energy constants from mixed-action lattice QCD*, *Phys.Rev.* **D86** (2012) 094509, [[1108.1380](#)].
- [134] [QCDSF 13] R. Horsley, Y. Nakamura, A. Nobile, P. Rakow, G. Schierholz et al., *Nucleon axial charge and pion decay constant from two-flavor lattice QCD*, *Phys. Lett.* **B732** (2014) 41–48, [[1302.2233](#)].
- [135] G. Colangelo and S. Dürr, *The pion mass in finite volume*, *Eur. Phys. J.* **C33** (2004) 543–553, [[hep-lat/0311023](#)].
- [136] PARTICLE DATA GROUP collaboration, K. A. Olive et al., *Review of Particle Physics*, *Chin. Phys.* **C38** (2014) 090001 and 2015 update.
- [137] V. Gülpers, G. von Hippel and H. Wittig, *The scalar radius of the pion from lattice QCD in the continuum limit*, *Eur. Phys. J.* **A51** (2015) 158, [[1507.01749](#)].
- [138] V. Gülpers, G. von Hippel and H. Wittig, *The scalar pion form factor in two-flavor lattice QCD*, *Phys. Rev.* **D89** (2014) 094503, [[1309.2104](#)].
- [139] [JLQCD/TWQCD 09] S. Aoki et al., *Pion form factors from two-flavor lattice QCD with exact chiral symmetry*, *Phys. Rev.* **D80** (2009) 034508, [[0905.2465](#)].
- [140] [CERN-TOV 06] L. Del Debbio, L. Giusti, M. Lüscher, R. Petronzio and N. Tantalo, *QCD with light Wilson quarks on fine lattices (I): first experiences and physics results*, *JHEP* **02** (2007) 056, [[hep-lat/0610059](#)].
- [141] [JLQCD 15A] S. Aoki, G. Cossu, X. Feng, S. Hashimoto, T. Kaneko, J. Noaki et al., *Light meson electromagnetic form factors from three-flavor lattice QCD with exact chiral symmetry*, *Phys. Rev.* **D93** (2016) 034504, [[1510.06470](#)].
- [142] [JLQCD 14] H. Fukaya, S. Aoki, S. Hashimoto, T. Kaneko, H. Matsufuru and J. Noaki, *Computation of the electromagnetic pion form factor from lattice QCD in the ϵ regime*, *Phys. Rev.* **D90** (2014) 034506, [[1405.4077](#)].
- [143] [PACS-CS 11A] O. H. Nguyen, K.-I. Ishikawa, A. Ukawa and N. Ukita, *Electromagnetic form factor of pion from $N_f = 2 + 1$ dynamical flavor QCD*, *JHEP* **04** (2011) 122, [[1102.3652](#)].
- [144] [LHP 04] F. D. R. Bonnet, R. G. Edwards, G. T. Fleming, R. Lewis and D. G. Richards, *Lattice computations of the pion form factor*, *Phys. Rev.* **D72** (2005) 054506, [[hep-lat/0411028](#)].

- [145] [QCDSF/UKQCD 06A] D. Brömmel et al., *The pion form factor from lattice QCD with two dynamical flavours*, *Eur. Phys. J.* **C51** (2007) 335–345, [[hep-lat/0608021](#)].
- [146] S. R. Amendolia et al., *A measurement of the space-like pion electromagnetic form factor*, *Nucl. Phys.* **B277** (1986) 168.
- [147] S. Dürr, *Validity of ChPT - is $M_\pi=135$ MeV small enough?*, *PoS LATTICE2014* (2015) 006, [[1412.6434](#)].
- [148] S. Dürr, *M_π^2 versus m_q : comparing CP-PACS and UKQCD data to chiral perturbation theory*, *Eur. Phys. J.* **C29** (2003) 383–395, [[hep-lat/0208051](#)].
- [149] N. H. Fuchs, H. Sazdjian and J. Stern, *How to probe the scale of $\bar{q}q$ in chiral perturbation theory*, *Phys. Lett.* **B269** (1991) 183–188.
- [150] J. Stern, H. Sazdjian and N. H. Fuchs, *What π - π scattering tells us about chiral perturbation theory*, *Phys. Rev.* **D47** (1993) 3814–3838, [[hep-ph/9301244](#)].
- [151] S. Descotes-Genon, L. Girlanda and J. Stern, *Paramagnetic effect of light quark loops on chiral symmetry breaking*, *JHEP* **01** (2000) 041, [[hep-ph/9910537](#)].
- [152] V. Bernard, S. Descotes-Genon and G. Toucas, *Chiral dynamics with strange quarks in the light of recent lattice simulations*, *JHEP* **1101** (2011) 107, [[1009.5066](#)].
- [153] [NPLQCD 06] S. R. Beane, P. F. Bedaque, K. Orginos and M. J. Savage, *f_K/f_π in full QCD with domain wall valence quarks*, *Phys. Rev.* **D75** (2007) 094501, [[hep-lat/0606023](#)].
- [154] D. Boito, A. Francis, M. Golterman, R. Hudspith, R. Lewis, K. Maltman et al., *Low-energy constants and condensates from ALEPH hadronic τ decay data*, *Phys. Rev.* **D92** (2015) 114501, [[1503.03450](#)].
- [155] P. A. Boyle, L. Del Debbio, N. Garron, R. J. Hudspith, E. Kerrane, K. Maltman et al., *Combined NNLO lattice-continuum determination of L_{10}^r* , *Phys. Rev.* **D89** (2014) 094510, [[1403.6729](#)].
- [156] [RBC/UKQCD 09] P. A. Boyle, L. Del Debbio, J. Wennekers and J. M. Zanotti, *The S Parameter in QCD from Domain Wall Fermions*, *Phys.Rev.* **D81** (2010) 014504, [[0909.4931](#)].
- [157] [JLQCD 08A] E. Shintani et al., *S -parameter and pseudo-Nambu-Goldstone boson mass from lattice QCD*, *Phys. Rev. Lett.* **101** (2008) 242001, [[0806.4222](#)].
- [158] J. Bijnens and P. Talavera, *Pion and kaon electromagnetic form-factors*, *JHEP* **0203** (2002) 046, [[hep-ph/0203049](#)].
- [159] M. Davier, L. Girlanda, A. Hocker and J. Stern, *Finite energy chiral sum rules and tau spectral functions*, *Phys.Rev.* **D58** (1998) 096014, [[hep-ph/9802447](#)].
- [160] C. Jung, *Status of dynamical ensemble generation*, *PoS LAT2009* (2009) 002, [[1001.0941](#)].